McKenzie, J.A., Davies, P.J., Palmer-Julson, A., et al., 1993
Proceedings of the Ocean Drilling Program, Scientific Results, Vol. 133

48. A SUMMARY OF INTERSTITIAL-WATER GEOCHEMISTRY OF LEG 133[1]

Peter K. Swart,[2] Alex Isern,[3] Harry Elderfield,[4] and Judith A. McKenzie[3]

ABSTRACT

The chemical compositions of the interstitial pore-water samples measured on board the *JOIDES Resolution* are compared with shore-based analyses of the samples' strontium, oxygen, and carbon isotopic compositions. These analyses support conclusions of large-scale water movement through the sediment overlying the Queensland Plateau at Sites 811, 812, 813, and 814, possibly leading to massive platform dolomitization.

At the Queensland continental margin sites, complete sulfate reduction and abundant methanogenesis occurs, yet little evidence of these processes is seen in the $\delta^{13}C$ of the pore waters. The failure to observe these signatures is a consequence of large-scale recrystallization of carbonate sediments masking the isotopic signatures of these processes. Although abundant igneous material is present at these sites, we do not think that significant alteration of these minerals is taking place in situ. Decreases in the Mg^{2+} and Ca^{2+} concentration result from the formation of dolomite and calcite; decreases in K^+ are a consequence of absorption onto clays; and decreases in the $\delta^{18}O$ are caused by carbonate recrystallization, with perhaps some minor influence from the alteration of volcanic glass.

At several sites there is evidence of diffusion of saline fluids from an underlying source, presumably evaporitic in nature, but this cannot be confirmed using either Sr or O isotopic data.

INTRODUCTION

During Leg 133 of the Ocean Drilling Program (ODP), sediments were cored in three different areas off the northeastern coast of Australia. All of these areas contained periplatform sediments (Schlager and James, 1978). This type of sediment is generally found near shallow-water carbonate platforms and consists of mixtures of metastable minerals, high-Mg calcite (HMC), and aragonite, as well as low-Mg calcite (LMC). The first area includes those sites (811, 812, 813, 814, 816, 817, 818, 824, 825, and 826) situated on submerged carbonate platforms or on the flanks of such platforms: the Queensland and the Marion plateaus (Fig. 1). The mineralogy of the sediments at these sites is predominantly carbonate, containing only small concentrations of noncarbonate minerals such as quartz and clay minerals. The second group of sites (815 and 823) is situated in the deeper water troughs between the Queensland and the Marion plateaus and the Great Barrier Reef (Fig. 1). These sites penetrated thick sequences of mixed carbonates (predominantly LMC) and siliciclastics. The third group (Sites 821, 820, 819, and 822) forms a proximal-to-distal transect from the Great Barrier Reef into the adjacent Queensland Trough (Fig. 1). This third group is situated in shallower water than is the second group and contains substantial concentrations of periplatform sediments mixed with quartz, feldspar, and clay minerals.

The aim of this paper is to synthesize the shipboard chemical data with oxygen and carbon isotopic analyses of pore waters, and to integrate them with data presented by Swart (this volume) and Elderfield et al. (this volume).

METHODS

The chemical data discussed in this paper have been presented in other papers, and, therefore, the reader is referred to these references for the appropriate analytical techniques: Davies, McKenzie, Palmer-Julson, et al. (1991); Elderfield et al. (this volume); and Swart (this volume). The C and O isotopic data for the pore waters, which have not been presented previously, were obtained using the methods described in Swart (this volume).

RESULTS

A summary of all geochemical data, including the Sr, C, and O isotopic data as well as measured shipboard data (with the exception of ammonia, phosphate, and silica), is shown in Table 1. As a result of some analytical problems, C and O isotopic data are not available for all samples.

Oxygen Isotopic Data

Sites 811, 812, 813, and 816

These sites are characterized by relatively heavy oxygen isotopic compositions in their pore waters throughout the cores (Fig. 2 and Table 1). Generally, these isotopic values lie between +0.5‰ and +1.0‰. Site 813 exhibits slightly depleted isotopic values relative to Sites 811 and 812, with $\delta^{18}O$ values lying between +0.2‰ and +0.5‰.

Sites 819, 820, 821, 822, and 823

These sites show an enrichment in their $\delta^{18}O$ values in the upper 50 to 100 mbsf, followed by a depletion down the core. The magnitude of this depletion increases with distance from the continental margin. The most depleted $\delta^{18}O$ values of –0.97‰ are reached in the sediments of Site 822 at a depth of 397.50 mbsf (Fig. 3 and Table 1). Site 823, which is actually the farthest away from the continental margin, reaches a minimum of only –0.5‰ at a depth of approximately 400 mbsf. From this depth toward the base of the core at 1000 mbsf, the isotopic composition increases to +0.5‰ (Fig. 4).

[1] McKenzie, J.A., Davies, P.J., Palmer-Julson, A., et al., 1993. *Proc. ODP, Sci. Results,* 133: College Station, TX (Ocean Drilling Program).

[2] Marine Geology and Geophysics, Rosenstiel School of Marine and Atmospheric Science, University of Miami, 4600 Rickenbacker Causeway, Miami, FL 33149-1098, U.S.A.

[3] Geologisches Institut, Eidgenossische Technische Hochschule, Sonneggstrasse 5, CH-8092, Zurich, Switzerland.

[4] Dept. of Earth Science, University of Cambridge, Downing St., Cambridge CB2 3EQ, United Kingdom.

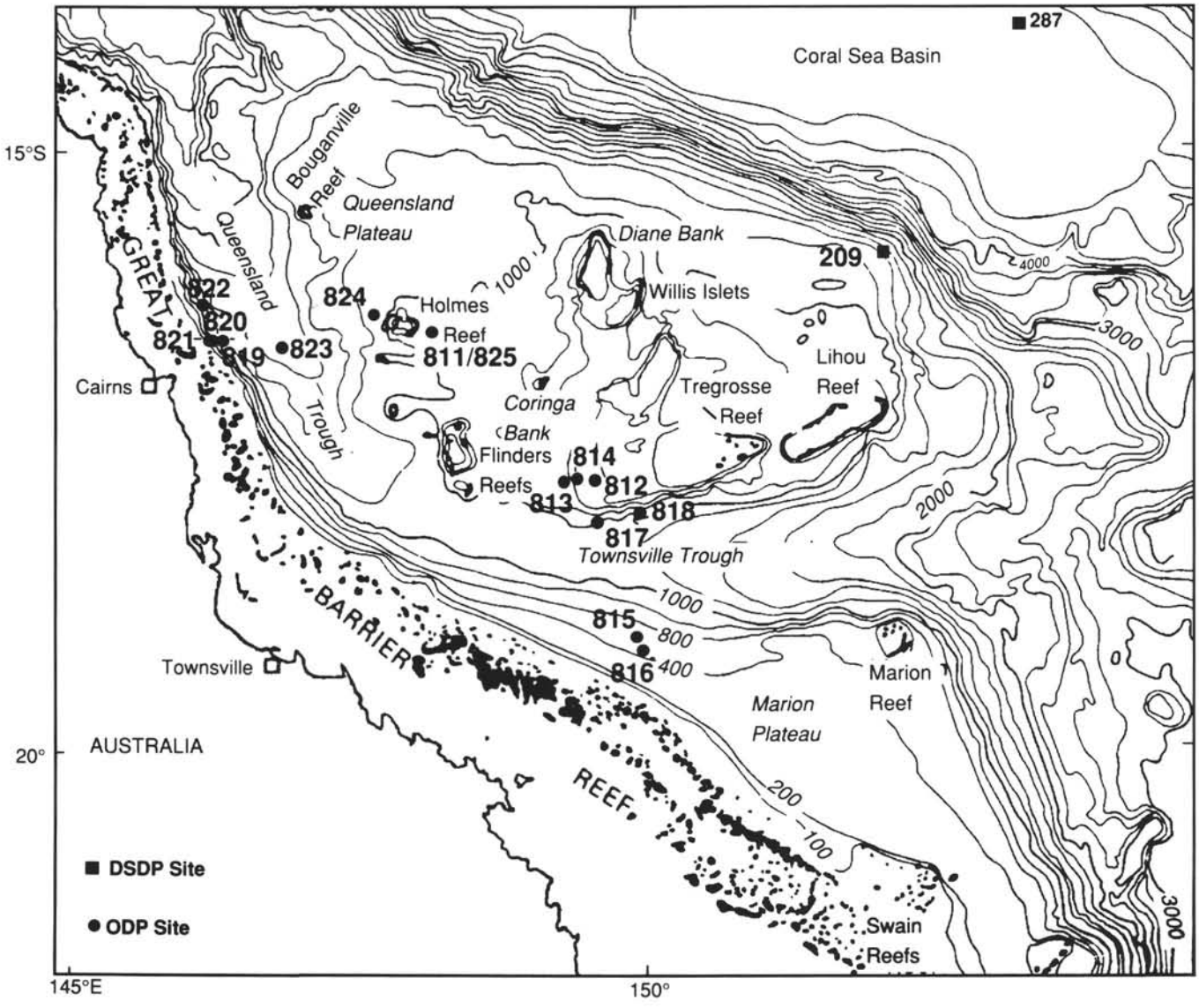

Figure 1. Location of the sites drilled during Leg 133.

Site 815

This site exhibited relatively heavy O isotopic compositions (0.5‰ to 1.2‰) throughout the cored interval (Fig. 5 and Table 1).

Carbon Isotopic Data

Sites 811, 812, 813, and 814

With the exception of the upper portion of Sites 814 and 812, these sites all exhibit slightly negative (–1‰) carbon isotopic compositions throughout (Fig. 6). Site 811 exhibits a slight enrichment down the core.

Sites 819, 820, 821, 822, and 823

All sites show a rapid depletion in $\delta^{13}C$ in the upper 10 to 50 mbsf, followed by an enrichment down the core. Site 819 exhibits the most severe depletion, attaining a $\delta^{13}C$ value of –15‰ at a depth of 25.48 mbsf. These depletions are less pronounced at other sites nearer to the Great Barrier Reef. In the lower portion of the core the $\delta^{13}C$ of the dissolved inorganic carbon (DIC) becomes isotopically heavier. The greatest enrichment occurs at Site 822, where values as heavy as +4‰ are reached. The magnitude of the enrichment in the lower portion of the core also changes with respect to the reef margin, being the highest at the sites farthest away from the margin (Fig. 7). In contrast to Site 822, Site 823 does not exhibit any enrichment in $\delta^{13}C$ down the core (Fig. 4 and Table 1).

Site 815

Site 815 exhibits a decrease in $\delta^{13}C$ throughout the upper 50 mbsf and maintains approximately the same isotopic composition to a depth of 350 mbsf. A slight enrichment is seen at the base of the core (Fig.5).

DISCUSSION

Carbonate Platform and Flank Sites 811/825, 812, 813, 814, 816, 817, and 818

The carbonate platform and flank sites can be separated into those situated on the Queensland Plateau and those located on the Marion Plateau. Sites 811, 812, 813, 814, 824, and 825 were cored on the Queensland Plateau and are all characterized by the present-day flux of substantial quantities of periplatform sediments (admixtures of bank-derived aragonite, HMC, and pelagic LMC). Sites 817 and 818

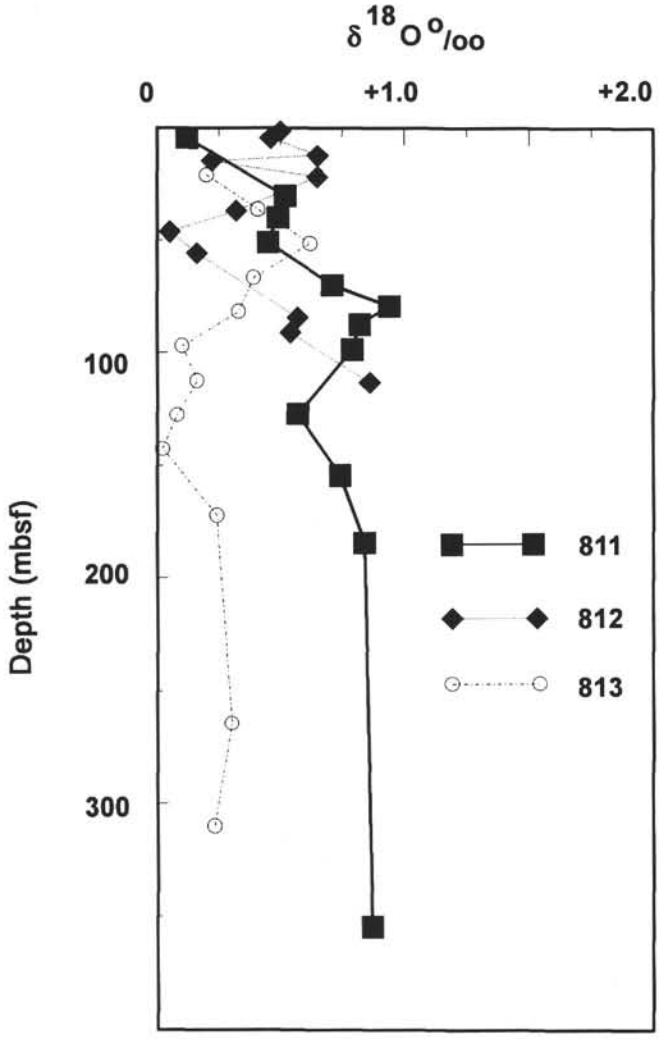

Figure 2. Oxygen isotopic data from pore waters recovered from Sites 811, 812, and 813.

were cored on the flanks of the Queensland Plateau. Sites 816 and 826 were drilled on the Marion Plateau.

Strontium

Previous ODP sites in the Bahamas (Leg 101) and the Maldives (Leg 115) where periplatform sediments have been cored (Swart and Guzikowski, 1988; Swart and Burns, 1990) were characterized by relatively high concentrations of Sr^{2+} in their interstitial pore fluids that resulted from the recrystallization of aragonite and HMC to LMC, and the consequent release of Sr^{2+} (Fig. 8). Therefore, perhaps the most surprising feature concerning the pore-water chemistry at Sites 811, 812, 813, and 814 is the absence of large increases in Sr^{2+} in the pore fluids, despite the fact that aragonite disappears relatively quickly with increasing depth sub-bottom (Fig. 9). We propose that fluid movement through the sediment prevents the establishment of normal diffusive Sr^{2+} gradients at these sites, an interpretation that can be supported by the following evidence: (1) the absence of geochemical gradients in the pore fluid; (2) the $^{87}Sr/^{86}Sr$ ratio of the pore water; and (3) the geothermal gradients. Perhaps the most persuasive evidence is the $^{87}Sr/^{86}Sr$ ratio of the pore fluid. The pore fluids from Sites 811 to 814 all have $^{87}Sr/^{86}Sr$ ratios that are much more radiogenic than the ratio of contemporaneous sediments and probably reflect mixing between Sr released by recrystallization of carbonate sediments and Sr^{2+} contributed from modern seawater circulating through the platform (Elderfield, this volume) (Fig. 10). Such circulation does not appear to be taking place at a similar depth in the deeper flank sites, Sites 817 and 818, or at Site 816 situated on the top of the Marion Plateau. These sites exhibit steep diffusive Sr^{2+} gradients (Fig. 11B) and $^{87}Sr/^{86}Sr$ profiles (Elderfield et al., this volume) similar to those described for oceanic sediments (Gieskes et al., 1986) (Fig. 11A).

Oxygen and Carbon Isotopes

Although not conclusive, the oxygen and carbon isotopic profiles of these sites support the hypothesis of fluid movement in that there is little evidence for significant carbonate recrystallization. For example, if the pore fluids were being strongly influenced by carbonate recrystallization, they would rapidly become isotopically depleted in oxygen. This is not the case. Instead, the oxygen isotopic compositions of the pore fluids are relatively heavy throughout (Fig. 2). Carbon isotopic compositions are lighter than surface seawater but presumably similar to bottom water for the area (Fig. 6). If these fluids were being affected by carbonate recrystallization, they probably would show heavier carbon isotopic compositions. In fact, both Sites 812 and 814 exhibit some isotopically heavy values in the upper portion of the core, the same interval that exhibits Sr^{2+} enrichment. Site 811 displays a progressive enrichment down the core. These values suggest the presence of carbonate reactions in these regions, and, possibly, the presence of different aquifers. Different aquifers in the carbonate platform also are suggested by these oxygen isotopic data.

Calcium and Magnesium

Of further interest is the nature of the Ca^{2+}, Mg^{2+}, and Cl^- gradients. Sites 813 and 814 are characterized by steep Ca^{2+} gradients near the sediment/water interface, but relatively constant concentrations as depth increases sub-bottom. In contrast, Site 812 exhibits a constant concentration of Ca^{2+} as depth increases and a relatively sudden increase in Ca^{2+} concentration from 80 to 120 mbsf (Fig. 9). Normally, the geochemical gradients observed at Sites 813 and 814 are indicative either of fluid movement out of these sediments or of horizontal flow parallel to the seafloor. In contrast, the gradients at Site 812 are associated with the movement of normal seawater into the formation, either vertically from the overlying seawater or in a horizontal direction. Hence, these gradients support the interpretation of fluid flow through the Queensland Plateau sites. At Sites 816, 817, and 818, Ca^{2+} gradients do not support fluid movement and, therefore, concur with the Sr^{2+} data.

Geothermal Gradients

The interpretation of fluid flow at the Queensland Plateau sites is supported by geothermal measurements performed during the logging of Sites 812 and 814. Site 812 shows a relatively constant temperature of approximately 11°C to a depth of 200 mbsf and then a sudden rise to a temperature of approximately 17°C. At Site 814 there is a sharp temperature gradient close to the seawater/sediment interface. One problem with these data is that they were taken by logging immediately after drilling, and there is a considerable probability that the geothermal gradients are not representative of those normally present. Problems with these data can be seen when comparing Sites 817 and 812, which exhibit similar geothermal gradients in the open logged hole, yet have clearly different interstitial pore-water profiles. Both of these sites probably penetrated under pressured zones, causing water to flow into the hole after logging. In the case of Site 812, this zone is probably close to the surface, thereby influencing water flow through the overlying veneer of uncemented sediments. At Site 817, however, this zone was considerably deeper;

Table 1. Summary of interstitial pore-water data from Leg 133.

Sample	Depth	Age	Ph	Alk (mM)	Sal (g/kg)	Cl^- (mM)	Mg^{2+} (mM)	Ca^{2+} (mM)	$SO_4$2- (mM)	K+ (mM)	Na^+ (mM)	Rb^{2+} (µM)	Sr (µM)	C (‰)	O (‰)	$^{87}Sr/^{86}Sr$	Error 1σ
825 Seawater	0.00	0.00	7.95	2.224	35.2	550	53.40	10.57	28.90				96				
825A-2W-1, 0–7	50.00	0.83	7.65	2.593	36.0	560	48.14	16.68	30.16				115	0.22			
825A-3W-1, 0–7	100.00	1.66	7.43	2.818	36.0	558	48.33	16.65	30.17				116	–0.34			
825A-4W-1, 0–7	150.00	2.49	7.63	2.634	35.8	556	48.35	16.63	30.27				118	0.37			
825A-5H-5, 145–150	207.45	3.45	7.44	2.591	35.8	561	47.82	16.68	29.22				113	0.35	1.51		
825A-8H-5, 140–150	235.95	9.25	7.44	2.300	36.0	561	48.02	16.57	30.16				110		1.67		
825A-10X-2, 140–150	250.45	12.20	7.45	2.950	35.8	561	48.45	16.54	30.38				111	–1.69	1.60		
811A-1H-5, 145–150	4.45	0.40	7.57	3.106	36.0	543	49.80	13.80	28.80				149		0.12		
811A-2H-5, 145–150	12.95	1.15	7.13	3.104	36.3	551	47.68	16.06	28.46				167				
811A-3H-5, 145–150	22.45	2.00	7.31	2.920	35.9	555	48.78	16.32	28.25				240				
811A-4H-5, 145–150	30.45	2.29	7.19	2.673	36.0	555	48.38	16.43	29.21				119		0.52		
811A-5H-5, 145–150	39.95	2.64	7.14	2.547	36.0	557	48.40	16.42	28.86				114		0.49		
811A-6H-5, 145–150	50.95	3.05	7.10	2.546	36.1	552	48.42	16.56	29.42				115		0.45		
811A-7H-5, 145–150	60.45	3.39	7.09	2.489	36.0	556	48.72	16.26	28.92				117				
811A-8H-5, 145–150	69.95	3.45	7.19	2.549	36.0	551	49.07	16.70	29.71				114	–0.80	0.71		
811A-9H-5, 145–150	79.45	4.00	7.13	2.549	36.0	557	48.82	16.56	29.51				115	–1.03	0.94		
811A-10H-5, 145–150	87.45	4.55	7.14	2.531	35.9	555	48.01	16.57	29.38				112	–0.99	0.82		
811A-11H-5, 145–150	98.45	5.60	7.12	2.605	36.0	557	48.66	16.24	29.50				119	–0.90	0.79		
811A-14H-5, 145–150	126.95	7.00	7.36	2.483	35.8	555	49.09	16.38	29.20				99	–0.23	0.57		
811A-17H-5, 145–150	153.95	7.60	7.40	2.391	36.0	542	50.39	16.40	29.72				112	–0.61	0.74		
811A-20H-5, 145–150	183.95	9.00	7.43	2.505	36.0	547	48.18	16.66	29.27				111	-0.24	0.84		
811B-8V-5, 145–150	354.45	19.00	7.45	3.219	36.0	557	48.88	16.71						0.32	0.87		
812A Surface seawater	0.00	0.00	7.96	2.543		551	54.01	10.36	29.62				91			0.709168	0.000000
812A-1H-2, 145–150	1.45	0.08	7.72	3.176	35.8	540	52.70	10.54	29.62				110	–0.32	0.50	0.709168	0.000032
812C-1H-5, 145–150	4.45	0.27	7.56	2.904	35.0	543	53.38	10.35	28.72				102	–0.32	0.46	0.709103	0.000062
812A-2H-5, 145–150	12.35	0.69	7.42	3.212	35.8	545	53.13	10.43	29.32				114	–0.28	0.65		
812C-2H-5, 145–150	14.80	0.90	7.42	2.886	35.0	539	53.16	10.32	29.62				114		0.22	0.000078	
812A-3H-5, 145–150	21.85	1.35	7.28	3.189	35.8	555	54.24	10.34	30.74				118		0.65		
812C-3H-5, 145–150	24.37	1.51	7.31	2.871	35.0	542	53.01	10.46	29.85				114			0.709083	0.000038
812C-5H-5, 145–150	36.97	2.31	7.43	2.701	35.2	542	52.85	10.32	29.62				102	0.39	0.32	0.709185	0.000028
812C-6H-5, 145–150	46.47	2.91	7.37	2.834	35.0	541	52.79	10.62	29.06				102		0.05	0.709168	0.000030
812C-7H-5, 145–150	55.97	3.51	7.27	2.900	35.0	543	52.50	10.51	29.70				102	–0.37	0.16	0.709184	0.000028
812C-8H-5, 145–150	64.47	4.05	7.35	2.902	35.2	543	52.62	10.79	29.19				102	–0.78	0.84	0.709173	0.000052
812C-9H-5, 145–150	74.97	4.71	7.34	2.863	35.2	534	52.86	10.62	29.66				102	–0.27		0.709136	0.000078
812C-10H-5, 145–150	84.47	5.31	7.30	2.908	35.2	543	52.09	10.84	27.61				102	0.35	0.57	0.709139	0.000038
812A-12X-5, 145–150	91.05	5.73	7.27	3.107	35.8	546	52.41	10.99	30.02				112		0.54	0.709158	0.000060
812C-13H-5, 145–150	112.97	7.12	7.45	2.910	35.2	541	52.38	11.42	29.03				102		0.86		
813A Seawater	0.00	0.00	7.99	2.455	36.2	545	54.46	10.46	29.89				96				
813A-1H-3, 145–150	4.45	0.28	7.67	3.135	35.0	545	51.93	11.77	30.67				134	–0.21		0.709149	0.000042
813A-2H-5, 145–150	13.17	0.45	7.34	2.927	36.0	548	52.66	11.45	29.24				111		0.20		
813A-3H-5, 145–150	22.67	0.93	7.17	2.501	35.8	543	51.95	11.30	30.55				107		0.41	0.709147	0.000024
813A-4H-5, 145–150	32.17	1.27	7.27	2.506	35.2	540	51.31	11.22	28.64				104		0.62	0.709147	0.000020
813A-5H-5, 145–150	41.67	1.88	7.16	2.679	35.5	546	51.82	11.18	29.38				105		0.39	0.709150	0.000024
813A-6H-5, 145–150	51.17	2.42	7.07	3.199	35.8	542	51.52	11.09	29.04				104	–1.17	0.33		
813A-7H-5, 145–150	60.67	2.50	7.28	2.187	35.2	542	51.86	11.15	29.83				105	–1.09	0.10	0.709137	0.000032
813A-8H-5, 145–150	70.17	2.60	7.30	2.200	35.2	540	52.06	11.26	29.47				105	–1.00	0.16	0.709137	0.000018
813A-9H-5, 145–150	79.67	3.00	7.31	2.584	35.2	540	51.90	11.18	29.05				105	–1.06	0.08	0.709194	0.000038
813A-10H-5, 145–150	89.17	3.51	7.21	2.557	35.2	543	51.73	11.27	29.84				110	–0.63	0.02	0.709138	0.000020
813A-12H-5, 145–150	107.47	5.00	7.43	2.767	35.2	542	50.99	12.10	29.91				101	–1.00	0.24	0.709124	0.000030
813A-15H-5, 145–150	136.67	7.00	7.34	2.776	35.2	538	51.08	11.94	28.51				99	–0.92			
813A-18H-5, 145–150	165.17	7.50	7.36	2.608	35.2	543	51.02	11.99	29.76				99	–1.22	0.30		
813A-21H-5, 145–150	193.67	9.50	7.62	2.755	35.2	544	51.15	11.86	31.20				99	–0.66	0.23		
814 Seawater	0.00	0.00			36.2	540	54.34	10.34	28.16				96			0.709163	0.000020
814A-1H-3, 145–150	4.45	0.28	7.47	3.900	35.5	519	53.62	10.35	29.08				167	–0.22		0.709173	0.000020
814A-2H-5, 145–150	13.37	0.47	7.31	3.260	35.0	544	53.42	10.78	28.37				181	0.35	–0.17	0.709165	0.000020
814A-3H-5, 145–150	22.87	0.93	7.18	3.196	35.2	539	53.83	11.02	29.25				167			0.709104	0.000028
814A-4H-5, 145–150	32.37	1.88	7.20	3.126	35.5	548	53.60	11.44	28.40				141	0.54		0.709125	0.000020
814A-5H-5, 145–150	41.00	2.42	7.16	3.123	35.5	546	53.14	11.83	28.70				125			0.709140	0.000024
814A-6H-5, 145–150	51.37	2.60	7.14	2.882	35.5	560	52.95	11.88	29.29				108	–0.28		0.709135	0.000020
814A-7H-2, 145–150	56.30	3.51	7.33	3.035	35.0	554	53.28	11.72	29.18				100			0.709174	0.000025
814A-9H-5, 145–150	73.97	6.27	7.52	3.139	35.2	538	53.09	11.51	28.59				95			0.709150	0.000024
814A-10H-5, 145–150	83.47	7.76	7.52	3.201	35.5	559	52.84	11.60	29.74				101	–0.48		0.709131	0.000028
814A-13H-5, 145–150	111.87	12.20	7.64	2.557	35.5	549	53.05	11.87	28.25				97	–0.65		0.709121	0.000018
814A-23X-1, 145–150	200.10	15.85	7.73	2.767	35.2	551	52.26	11.95	28.13				92	–0.69		0.709121	0.000020
814A-24X-2, 145–150	209.80	16.26	7.37	2.776	35.2	572	52.15	12.06	28.46				93	–1.21		0.709134	0.000028
814A-26X-3, 145–150	230.20	17.10	7.27	2.608	34.0	552	52.34	11.87	28.25				92	–0.44		0.709139	0.000020
814A-28X-2, 145–150	247.60	17.82	7.35	2.755	35.5	566	51.94	11.94	29.09				92	–1.10		0.709135	0.000020
814A-29X-2, 145–150	257.20	18.22	7.38	3.029	35.5	546	52.71	11.89	26.97				93	–1.00			
815A Surface seawater	0.00	0.00	8.24	2.646	35.0	573	53.55	10.27	28.12	9.80		1.4	86	0.11			
815A-2H-5, 145–150	14.25	0.47	7.28	3.082	35.5	537	48.59	10.28	24.16	10.84		1.4	335	–0.81	1.12		
815A-3H-5, 145–150	23.80	1.88	7.35	3.191	35.2	559	46.11	10.12	23.01	10.21		1.4	431	–0.98	0.73		
815A-4H-5, 145–150	33.25	2.42	7.32	3.414	35.8	573	44.56	10.15	20.09	9.82		1.4	526	–2.17	0.76		
815A-5H-5, 145–150	42.75	2.50	7.32	3.517	35.8	583	40.90	10.14	18.36	9.52		1.3	610	–2.34	1.23	0.708989	0.000021
815A-6H-5, 145–150	52.25	2.55	7.25	3.923	35.8	592	38.17	10.45	16.21	8.99		1.2	798	–2.41	0.62		
815A-7H-5, 145–150	61.75	2.60	7.21	4.046	36.0	596	35.37	10.85	14.75	8.75		1.1	817	–1.88	0.77		
815A-8H-5, 145–150	71.25	2.64	7.25	4.162	35.8	607	34.13	10.81	12.97	8.05		1.0	897	–2.08	0.85		
815A-9H-5, 145–150	80.75	2.67	7.32	4.408	36.0	613	32.37	10.75	11.26	7.71		1.0	973	–2.33	0.89		
815A-10H-5, 140–150	90.20	2.71	7.33	4.486	36.0	614	30.30	10.58	9.73	7.04		0.9	1063			0.709001	0.000038
815A-13H-5, 140–150	118.70	2.81	7.25	4.686	36.0	603	27.23	10.45	5.76	6.87		0.8	1239	–1.98	0.66		
815A-16H-5, 140–150	147.20	2.92	7.46	4.511	36.5	638	25.31	10.59	2.76	5.69		0.7	1347		0.72		
815A-19H-5, 140–150	175.70	3.02	7.43	4.318	37.8	663	25.44	11.16	1.63	5.54		0.6	1445	–1.62		0.708907	0.000021
815A-22H-5, 140–150	204.20	3.13	7.35	3.958	39.0	698	27.50	12.51	1.52	5.59		0.5	1534	–1.81	0.69		
815A-26X-3, 140–150	226.90	3.21	7.46	4.144	40.0	705	28.68	14.19	2.33	4.33		0.5	1541	–2.18	0.59	0.708897	0.000018
815A-28X-3, 140–150	246.20	3.28	7.56	4.005	40.0	699	30.54	15.24	4.11	4.62		0.5	1412	–2.57			

Table 1 (continued).

Sample	Depth	Age	Ph	Alk (mM)	Sal (g/kg)	Cl^- (mM)	Mg^{2+} (mM)	Ca^{2+} (mM)	$SO_4$2- (mM)	K+ (mM)	Na^+ (mM)	Rb^{2+} (µM)	Sr (µM)	C (‰)	O (‰)	$^{87}Sr/^{86}Sr$	Error 1σ
815A-31X-4, 140–150	276.70	3.39	7.38	3.218	42.0	714	31.96	20.19	5.69	4.67		0.5	1400	–2.14	0.53	0.708908	0.000021
815A-34X-5, 140–150	307.30	3.51	7.46	2.575	42.2	742	35.49	20.72	7.81	5.26		0.5	1414	–2.36	0.69		
815A-37X-5, 140–150	336.40	4.60	7.48	2.451	43.2	744	37.80	22.14	9.97	5.85		0.6	1261	–2.55			
815A-40X-5, 140–150	365.50	5.26	7.17	3.226	44.2	760	37.81	24.27	11.38	5.25		0.9	1342	–3.61	0.50		
815A-43X-5, 140–150	394.50	5.90	7.23	3.105	46.5	770	40.06	26.06	13.89	5.72		0.8	1124	–2.39	0.44	0.708864	0.000021
815A-47X-5, 140–150	432.70	6.74	7.26	3.107	45.5	760	42.61	26.82	15.99	6.43		1.1	920	–1.11			
816 Seawater	0.00	0.00	8.22	2.546	35.8	543	53.70	10.51	28.75				93	1.01			
816A-1H-3, 145–150	4.45	0.93	7.47	3.381	35.8	538	52.54	10.73	28.47				149	–0.55	0.32		
816A-2H-5, 145–150	11.95	1.88	7.22	3.000	35.8	548	51.64	11.58	29.60				210	–0.82	0.35		
816A-3H-5, 145–150	22.45	2.60	7.30	3.077	36.0	559	51.00	12.34	29.56				240	–1.70	1.40		
816A-4H-5, 145–150	31.95	3.50	7.28	3.306	36.4	562	50.60	13.09	29.46				297	–2.22	0.94		
816A-5H-5, 145–150	41.45		7.34	3.153	37.0	563	49.43	14.15	29.45				328	–1.44	1.04		
816A-6H-5, 145–150	50.95		7.24	3.240	37.5	571	49.06	14.98	29.01				336	–1.57	0.55		
816A-7H-2, 145–150	60.45		7.14	3.260	38.0	572	48.62	15.90	28.82				348	–1.51	0.54		
816A-8H-5, 145–150	69.95		7.25	3.058	37.8	584	48.42	16.65	28.39				349		0.65		
816A-9H-5, 145–150	79.45		7.26	3.038	37.0	572	47.62	17.00	27.95				318				
816A-10H-5, 145–150	88.95		7.39	3.173	36.5	562	49.18	15.13	29.31				223	–1.82	1.01		
817A-1H-3, 145–150	4.45	0.28	7.65	3.365	35.0	551	52.63	9.33	29.18				127		0.08		
817A-2H-5, 145–150	13.15	0.34	7.45	4.966	35.2	557	55.10	7.81	29.25				201				
817A-3H-5, 145–150	22.65	0.47	7.47	7.137	35.2	559	55.56	7.28	28.38				350		0.24		
817A-4H-5, 145–150	32.15	0.93	7.53	8.013	35.5	562	55.70	7.66	28.05				466				
817A-5H-5, 145–150	41.65	1.04	7.54	8.099	36.0	563	55.03	8.17	28.81				544			0.709138	0.000024
817A-6H-5, 145–150	51.15	1.16	7.32	7.898	35.5	559	54.49	8.19	29.05				517		0.45	0.709145	0.000026
817A-7H-1, 0–7	53.20	1.18	7.67	7.868	34.5	558	54.49	8.33	28.42				531				
817A-7H-5, 145–150	60.65	1.27	7.43	7.390	35.5	561	54.57	8.25	29.56				530		0.77		
817A-8H-5, 145–150	70.25	1.66	7.37	6.771	35.0	559	53.89	8.39	28.57				512			0.709118	0.000036
817A-9H-5, 145–150	79.65	2.04	7.37	6.545	35.0	557	54.08	8.61	29.16				500				
817A-10H-5, 145–150	89.15	2.42	7.34	6.127	35.2	562	54.01	9.02	28.78				475		0.14	0.709052	0.000024
817A-11H-5, 145–150	98.65	2.59	7.61	5.909	35.0	559	53.80	9.08	29.20				468				
817A-12H-1, 0–7	100.70	2.63	7.74	6.127	36.2	554	53.32	10.03	29.20				478		0.25		
817A-14H-5, 145–150	127.15	3.11	7.39	5.575	36.0	562	52.11	11.08	29.91				473				
817A-16H-5, 145–150	146.15	3.45	7.35	5.740	35.2	553	51.59	11.40	30.06				446		0.32	0.709016	0.000020
817A-17H-1, 0–7	148.20	3.88	7.43	6.065	35.8	555	51.52	12.00	29.20				472				
817A-19H-5, 145–150	174.62	4.60	7.50	5.443	35.5	558	50.61	13.26	30.13				432			0.708965	0.000020
817A-21H-5, 140–150	193.60	6.74	7.17	5.821	35.2	559	49.27	14.71	30.28				403		0.19	0.708916	0.000020
817A-22H-1, 0–7	195.70	6.97	7.62	4.600	35.5	558	50.06	14.72	31.06				393				
817A-24X-5, 140–150	222.10	10.48	7.29	4.729	35.5	565	49.31	15.72	29.98				382				
817A-26X-5, 140–150	241.40	13.00	7.39	4.376	36.0	563	48.39	16.41	30.55				367		0.03	0.708833	0.000018
817A-27X-1, 0–7	243.70	13.36	7.58	3.998	36.2	564	50.02	15.24	30.90				314				
817A-29X-5, 140–150	270.40	16.92	7.42	4.043	37.0	570	48.50	16.76	30.76				315		0.44	0.708824	0.000020
817A-5R-3, 140–150	303.40	17.00	7.26	3.908	37.5	575	46.51	19.27	30.00				365			0.708826	0.000030
818B Seawater	0.00	0.00	8.20	2.595	35.5	548	54.78	10.64	29.03				97			0.709173	0.000022
818B-1H-4, 145–150	4.49	0.28	7.46	3.488	34.8	535	52.94	10.03	27.33				196	0.29			
818B-2H-5, 145–150	12.99	0.48	7.59	3.232	35.0	537	53.61	9.99	27.98				211	0.94			
818B-3H-5, 145–150	22.46	0.58	7.30	4.699	36.2	540	54.82	8.79	27.72				449			0.709118	0.000040
818B-4H-5, 145–150	31.99	0.88	7.28	6.179	36.0	551	54.97	8.32	27.19				603			0.709144	0.000020
818B-5H-5, 145–150	41.49	0.93	7.30	6.373	36.0	555	54.30	8.61	26.57				662			0.709114	0.000030
818B-6H-5, 145–150	50.99	1.15	7.31	6.289		555	53.77	9.12	26.42				685	0.81			
818B-7H-5, 145–150	60.49	1.25	7.26	6.519	36.0	562	53.70	9.97	26.76				704			0.709067	0.000026
818B-8H-5, 145–150	69.99	1.48				562	61.97	11.04	26.93				716	0.39			
818B-9H-5, 145–150	79.49	1.68	7.72	6.679	36.2	564	52.45	11.24	26.66				685				
818B-10H-5, 145–150	88.99	1.88	7.38	6.497	36.2	572	52.61	11.42	26.56				746	0.78		0.709108	0.000028
818B-13H-5, 145–150	120.53	2.20	7.27	6.471	38.0	587	52.39	12.73	26.60				716			0.709036	0.000024
818B-16H-5, 145–150	148.91	2.40	7.24	6.269	38.2	606	52.50	13.44	27.59				704	0.24		0.709148	0.000064
818B-19H-5, 145–150	177.50	2.60	7.28	5.787	38.5	615	53.34	14.77	28.25				638	–0.77		0.709048	0.000020
818B-22H-5, 145–150	206.00	3.00	7.30	5.057	40.2	621	53.53	15.75	28.54				601			0.709055	0.000018
818B-25H-5, 145–150	234.51	3.20	7.24	4.412	40.2	634	53.46	18.32	29.83				599	–0.77		0.709032	0.000036
818B-28H-5, 145–150	262.00	3.51	7.29	3.413		620	51.68	21.29	32.21				470			0.709014	0.000018
818B-31H-5, 145–150	291.00	3.88	7.30	2.862		606	50.25	20.94	31.21				217	–0.55		0.708971	0.000021
819 Seawater	0.00	0.00	8.27	2.655	35.5	551	53.68	10.36	29.74	10.62	474		98	1.87			
819A-1H-5, 145–150	5.95	0.28	7.21	9.584	34.2	551	48.54	6.26	18.11	12.30	474		80	–12.32	0.48		
819A-2H-5, 145–150	15.95	0.32	7.31	10.926	32.5	550	39.39	4.16	6.97	10.08	476		95	–0.93	1.18		
819A-3H-5, 145–150	25.45	0.36	7.43	11.059	31.8	548	30.63	3.32	0.00	10.55	478		112	–15.00			
819A-4H-5, 145–150	34.95	0.39	7.33	9.500	31.8	550	25.42	4.95	0.00	9.33	487		179	–5.03			
819A-5H-5, 140–150	44.45	0.43	7.53	8.388	31.6	546	23.32	4.60	0.00	9.02	486		234	–1.83	0.66		
819A-6H-5, 140–150	53.95	0.47	7.40	7.652	30.5	542	19.79	4.35	0.00	8.22	490		273	–0.24	0.38		
819A-7H-5, 140–150	63.45	0.51	7.81	6.811	30.5	548	18.43	3.11	0.00	8.13	500		242	–0.34	0.66		
819A-8H-5, 140–150	72.90	0.55	7.68	7.936	31.0	535	16.83	3.45	0.00	7.18	491		221	0.06	0.28		
819A-9H-5, 140–150	82.40	0.58	7.53	8.341	31.0	541	16.05	3.41	0.00	7.02	499		241	0.05	0.12		
819A-10H-5, 140–150	91.90	0.62	7.84	8.985	31.0	539	15.26	2.86	0.00	6.79	501		231		0.35		
819A-13H-5, 140–150	118.40	0.73	7.88	9.988	30.2	548	13.89	2.97	0.00	5.64	514		292	–0.51	0.05		
819A-16H-6, 140–150	137.80	0.80	7.88	10.288	31.5	549	16.35	3.41	2.66	6.21	514		344	–0.16	–0.08		
819A-19X-2, 140–150	168.80	0.92	7.58	11.879	30.5	539	17.68	3.86	2.47	5.41	502		483	0.26	–0.08		
819A-23X-5, 140–150	205.50	0.93	7.71	12.423	31.0	537	18.61	4.42	1.27	4.82	497		260	1.56	–0.19		
819A-25X-1, 140–150	224.40	0.93	7.51	11.559	31.0	544	19.27	4.81	1.95	4.99	502		252	0.22	–0.29		
819A-28X-1, 140–150	243.30	0.97	7.67	10.122	31.0	541	25.37	5.81	6.23	5.15	491		171		–0.45		
819A-31X-2, 140–150	272.30	1.02	7.58	9.691	31.0	535	18.31	4.35	1.06	3.91	493		155	2.04	–0.31		
819A-34X-2, 140–150	301.30	1.07			31.0	534	22.07	5.50	3.06	3.62	478		277	0.28			
819A-37X-5, 140–150	330.30	1.13	7.72	9.745	31.0	544	17.69	4.63	0.34	3.43	502		174	1.87	–0.41		
819A-40X-6, 140–150	358.90	1.18	7.68	7.819	31.5	550	22.08	5.83	7.13	3.34	509		176	1.18	0.00		
819A-43X-5, 140–150	387.80	1.27	7.80	7.528	31.0	541	16.51	4.95	0.39	3.02	499		206	1.09	–0.47		
820 Seawater	0.00	0.00	8.10	2.574	35.0	556	52.50	10.56	29.39	10.68	480		114	1.20			
820A-1H-5, 145–150	7.45	0.06	7.47	6.384	35.0	555	53.80	8.39	24.91	10.20	476		103	–0.67			
820A-2H-5, 145–150	14.65	0.12	7.56	5.386	36.2	560	51.13	6.96	22.46	10.11	484		126	–7.83	0.27		
820A-3H-5, 145–150	24.15	0.20	7.52	5.501	34.0	562	43.31	6.88	16.62	9.41	491		175	–0.79			

Table 1 (continued).

Sample	Depth	Age	Ph	Alk (mM)	Sal (g/kg)	Cl^- (mM)	Mg^{2+} (mM)	Ca^{2+} (mM)	$SO_4$2- (mM)	K+ (mM)	Na^+ (mM)	Rb^{2+} (µM)	Sr (µM)	C (‰)	O (‰)	$^{87}Sr/^{86}Sr$	Error 1σ
820A-4H-5, 145–150	33.65	0.28	7.48	6.157	33.0	558	34.33	6.22	9.63	7.98	494		210	–1.69	0.55		
820A-5H-5, 145–150	43.15	0.31	7.41	6.490	32.0	554	27.07	5.20	3.46	7.51	494		241	–1.16	0.53		
820A-6H-5, 145–150	52.65	0.34	7.50	7.621	31.8	552	22.12	4.89	0.00	6.92	498		221	–1.42	0.53		
820A-7H-5, 140–150	62.10	0.37	7.94	7.901	31.8	555	20.69	4.62	0.80	6.36	507		227	–2.39			
820A-8H-5, 140–150	71.60	0.41	7.63	7.700	31.5	544	18.91	4.05	0.00	6.31	499		271	–1.10	0.43		
820A-9H-5, 140–150	81.10	0.44	7.44	7.348	30.5	539	15.76	3.55	0.00	5.65	501		318	–0.57			
820A-10H-5, 140–150	90.60	0.47	7.67	6.365	31.2	543	12.80	3.15	0.00	5.58	511		304	–0.44			
820B-12H-1, 0–7	103.20	0.53	7.79	6.652	31.0	540	14.80	3.53	3.23	5.50	510		331	–1.04	0.44		
820A-13H-5, 140–150	119.10	0.60	7.91	7.311	31.0	539	9.58	2.74	0.00	4.67	516		331		0.31		
820A-16V-1, 140–150	141.60	0.70	8.02	5.613	30.2	542	8.73	3.01	0.88	4.86	520		426		0.14		
820B-17X-1, 0–7	150.70	0.74	7.95	3.217	34.0	547	43.47	8.24	2.00	8.42	442		251				
820B-17X-3, 140–150	155.10	0.75	7.88	6.726	31.0	537	7.25	2.44	0.29	4.01	520		400		0.02		
820B-20X-5, 140–150	182.20	0.87	7.82	7.651	31.0	536	5.65	2.31	0.29	2.89	525		444	–0.71	–0.19		
820B-23X-1, 0–7	203.40	0.97	8.44	7.480	32.5	539	15.85	4.20	7.93	4.29	517		369		0.25		
820B-23X-2, 140–150	206.30	0.98	7.89	6.981	30.2	538	4.88	2.31	0.43	2.65	528		416	–0.92			
820B-27X-3, 140–150	246.20	1.16	7.89	6.214	30.2	540	3.89	1.80	0.36	2.25	532		471		0.18		
820B-28X-1, 0–7	251.10	1.18	8.16		31.0	551	16.01	4.74	9.90	3.25	525		473				
820B-30X-1, 140–150	271.80	1.27	7.94	5.382	31.8	550	11.20	4.32	5.86	3.08	532		421		0.54		
820B-33X-1, 0–7	299.40	1.32	8.29	3.902	35.0	536	44.96	9.38	26.47	7.47	476		353				
820B-33X-1, 140–150	300.80	1.32	8.23	6.604	30.0	535	5.77	2.81	0.00	2.03	521		554				
820B-36X-5, 140–150	335.90	1.39	8.14	5.716	30.5	542	9.05	2.94	2.62	2.43	525		504		0.97		
820B-39X-2, 140–150	360.40	1.44	8.00	6.356	31.8	536	9.25	3.48	3.54	2.58	520		642	–0.77			
820B-42X-4, 140–150	382.60	1.48	7.89	6.195	31.2	536	9.41	3.63	2.20	2.49	517		575		0.69		
821 Seawater	0.00	0.00	8.12	2.595	35.2	542	53.51	10.53	30.15	10.66	466		93	1.73			
821A-1H-2, 145–150	2.95	0.02	7.52	6.996	35.8	563	54.65	8.61	26.19	9.04	487		82	–7.69	0.76		
821A-2H-5, 145–150	11.85	0.10	7.40	7.160	35.2	561	54.11	6.25	23.54	9.37	485		86	–0.60	0.75		
821A-3H-5, 145–150	21.35	0.18	7.32	4.817	35.2	558	49.38	7.80	24.47	9.79	487		147	–0.69	1.10		
821A-4H-5, 145–150	30.85	0.28	7.59	5.086	35.2	560	44.40	8.05	21.73	9.04	494		222	–4.93	1.71		
821A-5H-5, 145–150	40.35	0.30	7.33	5.099	34.9	554	35.44	7.69	18.44	8.59	501		329	–0.33	1.54		
821A-6H-5, 145–150	49.85	0.33	7.45	5.267	33.8	551	29.74	6.14	15.65	6.08	509		353	0.89	1.95		
821A-7H-5, 140–150	59.30	0.37	7.29	6.047	33.5	551	24.85	5.96	13.29	6.38	515		379	–0.70	2.04		
821A-8H-5, 145–150	68.85	0.40	7.48	6.144	33.5	545	21.25	5.51	11.69	5.76	514		412	–0.56	1.14		
821A-9H-5, 145–150	78.35	0.43	7.40	5.382	33.0	548	18.46	4.91	11.17	5.15	523		437	0.24	0.39		
821A-10H-5, 145–150	87.85	0.46	7.68	5.887	32.0	544	15.58	4.43	9.22	5.21	522		436	–0.36	0.38		
821A-13H-5, 145–150	116.35	0.47	7.87	9.036	32.0	545	7.82	2.91	4.04	3.59	536		489	0.48	0.58		
821A-17X-5, 140–150	144.80	0.71	7.89	6.330	30.2	538	5.08	2.32	0.00	2.68	526		462	0.02	0.91		
821A-20X-5, 140–150	182.30	0.93	7.82	6.322	30.2	539	6.96	2.84	0.31	3.18	522		548	0.21	0.33		
821A-23X-5, 140–150	210.90	1.00	8.11	5.745	30.5	542	5.65	2.84	0.00	2.16	527		651	–0.64	0.30		
821A-26X-5, 140–150	239.60	1.13			30.5	538	5.26	2.88	0.44	1.79	520		759	–0.62	0.63		
821A-29X-5, 140–150	268.50	1.26	8.20	4.360	30.2	540	4.74	2.66	0.11	1.67	527		702	–0.48	0.50		
821A-33X-5, 140–150	307.10	1.33	8.23	5.266	32.2	536	7.56	3.29	1.60	1.82	520		612	–0.70	0.46		
821A-35X-3, 140–150	232.40	1.19	8.35	3.549	30.5	538	5.22	3.14	0.00	1.44	522		695				
821A-38X-5, 140–150	355.30	1.42	8.10	5.012	31.5	535	8.71	3.79	0.83	1.61	514		642	–0.97	0.39		
821A-41X-4, 140–150	382.70	1.48	8.33	3.650	30.2	538	6.87	4.03	1.33	1.41	517		730	–1.35	0.67		
822 Seawater	0.00	0.00	8.20	2.750	35.0	546	54.61	10.54	28.54	12.03			102	0.06			
822A-2H-5, 145–150	8.40	0.14	7.58	9.862	33.0	538	42.94	4.28	10.54	11.43			83		0.15		
822A-3H-5, 140–150	17.80	0.28	7.55	13.828	32.5	547	34.64	4.27	0.00	10.04			123	–1.82	0.33		
822A-4H-5, 140–150	27.30	0.47	7.63	12.057	32.0	544	31.57	4.61	0.00	9.70			140	–6.35	0.20		
822A-5H-5, 140–150	36.80	0.55	7.32	11.822	32.0	545	30.31	4.35	0.00	8.95			161		0.25		
822A-6H-5, 140–150	46.30	0.62	7.52	10.469	32.0	535	29.26	4.19	0.00	7.83			154	–5.85	0.09		
822A-7H-5, 140–150	55.80	0.70	7.46	10.910	32.0	530	27.89	3.99	0.00	6.04			146		0.27		
822A-8H-5, 140–150	65.30	0.78	7.45	8.561	31.0	533	26.22	4.48	0.00	7.77			140		0.11		
822A-9H-5, 140–150	74.80	0.85	7.72	9.270	31.8	543	26.83	3.96	0.00	8.08			138	0.26	0.77		
822A-10H-5, 140–150	84.30	0.93	7.12	9.092	31.8	537	26.59	3.88	0.00	7.37			140		0.95		
822A-11H-5, 140–150	93.80	0.95	7.62	9.498	31.5	543	26.05	3.95	0.00	6.40			137	1.16			
822A-12H-1, 0–7	95.90	0.95	7.70	3.571	35.0	563	49.48	9.39	26.88	5.60			166		0.39		
822A-14X-4, 140–150	122.80	1.01	7.68	10.575	32.0	536	24.72	4.62	0.00	6.16			142		0.01		
822A-17X-5, 140–150	151.70	1.07	7.47	10.686	32.0	540	25.69	5.41	1.24	5.41			136	3.27			
822A-18X-1, 0–7	154.00	1.08	8.12	5.981	34.0												
822A-20X-3, 140–150	177.70	1.13	7.73	8.703	31.0	536	23.51	4.49	0.00	5.06			126		–0.87		
822A-23X-1, 0–7	192.20	1.16	8.70	8.093	35.0												
822A-23X-2, 140–150	195.10	1.16	7.69	8.347	31.8	544	23.72	4.84	0.00	4.64			132		–0.72		
822A-27X-5, 140–150	247.60	1.27	7.86	8.571	31.2	550	23.18	5.32	1.02	4.44			118	2.33	–0.72		
822A-28X-1, 0–7	249.80	1.28	8.72	6.904	34.0	545	41.25	8.47	19.77	6.16			118				
822A-29X-5, 140–150	266.90	1.31	7.83	7.049	32.2	562	23.27	4.85	2.36	4.64			116	2.95	–0.70		
822A-32X-4, 140–150	294.30	1.37	7.82	8.388	31.5	545	22.74	5.94	1.12	3.38			158		–0.95		
822A-33X-1, 0–7	298.10	1.48	8.32	7.282	34.0	542	38.81	7.86	12.78	4.73			143				
822A-35X-4, 140–150	323.40	1.74	7.70	5.941	31.5	548	21.35	5.40	0.64	3.32			214		–0.89		
822A-38X-1, 0–7	346.30	1.98	8.27	4.178	34.2	545	40.09	9.29	21.47	5.20			187				
822A-38X-4, 140–150	352.20	2.04	7.82	4.846	31.5	547	18.10	5.83	1.48	3.37			264				
822A-41X-3, 140–150	379.50	2.33	7.69	5.769	31.8	551	21.22	5.65	3.45	3.14			290		–0.97		
822A-44X-4, 140–150	405.90	2.60	7.85	5.050	31.8	547	18.72	6.54	0.34	2.62			388		–0.91		
822A-47X-4, 140–150	430.20	2.85	7.90	4.215	31.8	547	15.42	6.73	0.95	2.10			487		–0.94		
823 Seawater	0.00	0.00	7.93	2.456	35.0	545	53.56	10.47	30.22	10.31	469		105			0.709160	0.000020
823A-1H-3, 145–150	4.45	0.14	7.51	4.421	35.0	543	52.11	9.31	26.80	11.42	466		133	–1.94	0.38	0.709165	0.000023
823A-2H-5, 145–150	13.25	0.21	7.35	4.635	35.0	546	50.94	8.81	26.96	11.94	472		148	–2.24	0.04		
823A-3H-5, 145–150	22.75	0.28	7.40	7.759	33.8	547	47.22	5.32	15.72	12.07	468		157	–3.84	0.89		
823A-4H-5, 145–150	32.25	0.47	7.50	9.881	32.5	543	39.00	3.13	6.93	11.43	469		190	–3.10	0.56		
823A-5H-5, 145–150	41.75	0.57	7.43	12.196	31.8	550	33.03	3.72	0.67	10.06	479		202	–7.24			
823A-6H-5, 145–150	51.25	0.66	7.43	12.011	32.2	550	31.36	4.10	0.00	9.74	479		218	–4.87	0.10	0.709155	0.000018
823B-7H-1, 0–7	55.80	0.71	8.01	12.550	31.8	545	31.55	4.12	0.00	8.24	475		241	–0.92			
823A-7H-5, 145–150	60.75	0.76	7.39	11.421	31.8	544	29.67	4.36	0.00	9.84	475		220	–2.39			
823A-8H-5, 145–150	70.25	0.85	7.43	10.354	31.8	556	28.10	4.12	0.00	12.67	487		221		0.06		
823A-9H-5, 145–150	79.75	0.93	7.52	9.538	32.0	547	28.18	3.52	0.00	10.05	480		201	–1.60	–0.14		
823A-10H-5, 145–150	89.25	1.03	7.78	8.922	31.8	547	27.61	3.39	0.00	9.95	480		196	–1.55			

Table 1 (continued).

Sample	Depth	Age	Ph	Alk (mM)	Sal (g/kg)	Cl^- (mM)	Mg^{2+} (mM)	Ca^{2+} (mM)	$SO_4$2- (mM)	K+ (mM)	Na^+ (mM)	Rb^{2+} (µM)	Sr (µM)	C (‰)	O (‰)	$^{87}Sr/^{86}Sr$	Error 1σ
823B-12H-1, 0–7	103.30	1.17	8.33	9.912	31.8	542	28.42	4.83	0.43	5.50	478		212				
823B-12H-5, 140–150	110.70	1.24	7.82	7.745	32.2	542	25.91	3.97	0.00	8.11	478		197	–1.85	0.13		
823A-13H-5, 145–150	117.95	1.27	7.87	7.929	31.8	545	25.18	3.97	0.00	8.24	483		216	–1.57	0.06		
823B-15X-5, 140–150	139.50	1.36	7.82	7.668	31.8	547	26.15	3.77	0.20	7.25	484		234	–0.41	0.04	0.709062	0.000024
823B-17X-1, 0–7	151.40	1.48	7.70	4.450	34.0	548	44.72	7.73	20.38	7.56	477		211	0.61			
823B-18X-3, 140–150	165.50	2.29	7.66	7.651	31.5	553	25.98	4.05	0.65	6.44	491		282				
823B-21X-3, 140–150	194.60	2.34	7.92	6.824	32.0	549	23.74	4.14	0.00	8.21	488		374	–0.72	–0.37		
823B-22X-1, 0–7	199.80	2.38	7.59	7.914	32.2	547	25.94	4.74	0.50	5.58	485		409				
823B-24X-2, 140–150	221.60	2.42	7.76	6.081	31.8	547	20.96	5.14	0.00	5.25	491		477	–1.16	–0.60	0.708990	0.000026
823B-26X-1, 0–7	237.70	2.60	8.03	6.822	33.8	543	27.50	5.20	4.32	4.31	485		505				
823B-27X-6, 140–150	256.20	2.65	7.86	5.968	31.8	548	21.41	3.81	0.00	4.73	494		432	–1.14			
823B-30X-2, 140–150	279.20	2.87	7.82	4.959	31.8	552	21.87	3.80	0.35	4.39	497		619		–0.30	0.708962	0.000018
823B-32X-1, 0–7	295.60	3.03	8.03	5.752	31.8	543	23.73	5.96	3.60	3.66	489		662				
823B-33X-4, 140–150	311.20	3.18	7.91	3.780	32.0	546	20.44	5.21	2.42	3.98	495		687	–2.52	–0.35		
823B-36X-5, 140–150	341.60	3.48	7.91	3.068	31.8	558	18.45	4.82	0.04	4.43	506		703	–0.85	–0.33		
823B-39X-5, 140–150	370.40	3.51	7.97	3.537	31.8	554	19.16	4.64	0.00	3.49	502		654	–1.18	–0.51	0.708878	0.000026
823B-42X-4, 140–150	397.90	3.70	7.84	3.893	31.8	551	18.67	5.73	0.45	2.95	499		742	–1.18	–0.50	0.708846	0.000040
823B-45X-5, 140–150	428.30	3.88	7.73	3.528	31.8	549	17.23	5.67	0.00	2.84	498		825	–3.03	–0.58	0.708840	0.000030
823B-48X-4, 140–150	455.80	3.95	7.70	2.950	31.8	556	15.81	6.16	0.19	2.60	508		1029	0.56	–0.11		
823B-52X-4, 140–150	493.70	4.15	7.83	2.838	31.8	560	13.26	7.41	0.00	2.45	514		1185	–1.59	–0.52	0.708855	0.000030
823B-55X-5, 140–150	525.20	4.24			32.0	557	12.99	7.91	0.00	1.70	508		1269	–1.64	–0.50	0.708878	0.000026
823B-58X-5, 140–150	552.80	4.40	7.87	2.431	32.0	560	13.12	8.43	0.48	1.69	513		1338		0.04	0.708904	0.000024
823B-61X-5, 135–150	581.65	4.50	7.72	2.335	32.2									–1.43		0.708879	0.000028
823B-64X-1, 135–150	604.55	4.60	7.91	2.081	32.2	563	13.71	9.00	1.08	2.27	513		1515	–1.51	–0.48	0.708850	0.000022
823B-67X-5, 135–150	639.55	5.06	7.90	1.836	32.2	571	14.18	9.29	0.69	2.25	519		1780		–0.42		
823B-70X-5, 110–125	667.70	5.26	7.81	1.897	32.2	568	13.42	10.27	1.20	2.33	515		1879		–0.37		
823B-73X-2, 135–150	692.45	5.40	7.87	1.910	32.2	572	14.40	10.75	1.14	2.44	515		1913		–0.15	0.708884	0.000034
823B-76X-4, 135–150	724.45	5.60	7.79	2.848	32.2	568	14.02	11.91	0.55	2.28	510		2248	–3.86		0.708879	0.000022
823B-79X-4, 135–150	753.45	5.90	7.70	2.680	32.4	572	14.54	13.42	1.37	2.65	511		2335		–0.17		
823B-82X-1, 135–150	778.05	6.31	7.56	3.181	32.5	568	16.60	12.24	1.96	2.13	507		2410		–0.11		
823C-1R-3, 130–150	788.30	6.48	7.91	2.258	32.5	569	17.15	12.25	2.60	3.10	507		2162	–2.22	–0.07		
823C-4R-1, 130–150	913.90	8.54			33.0	571	17.65	13.63	2.79	3.73	505		2023				
823C-7R-2, 130–150	844.50	7.40			33.8	566	18.95	14.70	2.92	3.75	495		2248		0.00		
823C-10R-1, 125–150	872.05	7.85			33.8	576	17.05	16.17	1.92	2.74	504		2444		0.16		
823C-13R-4, 130–150	905.50	8.40			35.0	576	16.60	17.70	1.78	2.34	501		2785		0.14		
823C-16R-4, 130–150	934.60	8.88			35.0	570	18.57	18.11	2.84	2.16	494		2774				
823C-19R-3, 130–150	961.60	9.33			34.0	577	20.33	19.77	3.97	2.88	495		2750		0.36	0.708819	0.000018
823C-22R-3, 130–150	990.50	11.60			33.8	570	21.88	18.00	5.63	3.68	491		2877		1.47	0.708804	0.000018
824 Seawater	0.00	0.00	7.99	2.745	35.2	556	54.87	10.44	29.41	10.30			110			0.709160	0.000020
824B-1H-2, 145–150	2.95	0.03	7.62	3.650	35.0	541	54.12	10.30	29.19	12.17			203	2.24	0.20	0.709142	0.000026
824B-2H-5, 145–150	12.45	0.12	7.37	3.406	35.5	541	54.72	10.06	29.62	10.81			323	0.78	0.19	0.709172	0.000026
824B-3H-5, 145–150	21.95	0.20	7.40	3.388	35.2	542	54.16	10.30	29.67	10.43			326		0.27	0.709192	0.000026
824B-4H-5, 145–150	31.45	0.29	7.60	2.994	35.2	542	54.11	10.26	29.73	10.17			249		0.24	0.709124	0.000036
824B-5H-5, 145–150	40.95	0.38	7.58	3.066	35.2	541	54.29	10.37	29.20	11.68			285			0.709107	0.000034
824B-6H-5, 145–150	50.45	0.47	7.41	3.064	35.2	539	53.97	10.45	29.00	10.35			208	0.84	0.10	0.709100	0.000032
824A-1H-5, 140–150	57.40	0.63	7.57	3.339	35.0	548	54.19	10.47	29.52	11.48			277	–0.60	0.20	0.709120	0.000022
824A-2H-5, 140–150	66.90	0.84	7.35	3.037	35.0	546	54.81	10.50	28.97	10.71			271			0.709108	0.000022
824A-3H-4, 140–150	74.90	1.02	7.29	3.375	35.0	541	54.29	10.46	30.00	9.85			270			0.709127	0.000044
824A-5H-5, 140–150	95.40	1.48	7.69	2.906	35.0	541	53.23	10.49	29.89	10.11			265	1.24		0.709111	0.000022
824A-8H-2, 140–150	119.40	2.00	7.62	3.100	35.0	546	53.83	10.67	29.38	10.26			280	1.22		0.709116	0.000018
824A-14H-5, 140–150	173.10	5.26	7.52	2.973	35.0	551	54.45	10.74	29.63	11.07			223		0.19	0.709112	0.000024
824A-17X-2, 145–150	195.50	6.00	7.63	3.106	35.8	556	55.58	10.74	30.47	11.89			212	0.24			
824A-21X-2, 140–150	235.60	8.00	7.65	3.062	35.8	560	55.68	10.79	29.96	11.30			234	1.11	–0.02	0.709090	0.000028

therefore, no significant vertical flow down through the sediments appears to be taking place. The actual geothermal gradient at Site 817 was measured in the sediments using the WSTP tool and found to be 57°C/km. In contrast, at Site 825/811, the gradient was slightly higher at 80°C/km.

In conclusion, although the temperatures obtained during logging do suggest the presence of over- and underpressured zones in the sediments, these data do not reflect the geothermal gradients actually present in the sediments and, therefore, cannot be taken to be indicative of water flow. The slight differences between Sites 825 and 817 indicate the presence of different geothermal gradients, which may be sufficient to induce circulation. To further confirm the presence of geothermally driven water flow, an extensive heat flow survey should be conducted over the Queensland Plateau.

Deep Trough Sites: 815 and 823

The overall geochemistry of Sites 815 and 823 is dominated by: (1) intense sulfate reduction and carbonate recrystallization in the upper portion of the sediment column; and (2) the increasing salinity of the pore fluids with increasing depth. At Site 815, the concentration of Ca^{2+} remains constant throughout the upper 200 mbsf. Throughout this same interval, the concentration of Mg^{2+} decreases to 26 mM, Sr^{2+} increases to 1400 µM, and SO_4^{2-} decreases to 2 mM. Below 200 mbsf, the concentration of all components, with the exception of Sr^{2+}, increases to the bottom of the core (473 mbsf). The decrease in Sr^{2+} occurs because of the increase in SO_4^{2-}, which in turn causes the mineral celestite to become supersaturated. In contrast, Site 823 penetrated 1103 mbsf and exhibits much more pronounced decreases in Ca^{2+}, Mg^{2+}, and K^+. Site 823 also contains a much lower carbonate content and, consequently, a higher concentration of clay minerals. Site 823 also exhibits an increase in the salinity of the pore fluids in the lower portions of the hole, but at a reduced rate compared with that at Site 815. The change in $\delta^{18}O$ from –0.5 to +0.5 is much greater at Site 823 than at Site 815, which possesses heavy oxygen isotopic values throughout.

It has been suggested that the general increase in chlorinity at Sites 815 and 823 resulted from the diffusion of salts from an underlying evaporite unit (Davies, McKenzie, Palmer-Julson, et al., 1991). Increases in Cl^- also were observed at Sites 817, 818, and 822 (Fig. 12). Such a common trend suggests that perhaps the evaporitic unit postulated to underlie Sites 815 and 823 may be an extensive feature of the Queensland Trough. Such a deposit has not as yet been identified in the Townsville Trough, but is known in sediments of Oligocene age in the Capricorn Basin approximately 100 km to the south (Ericson, 1976).

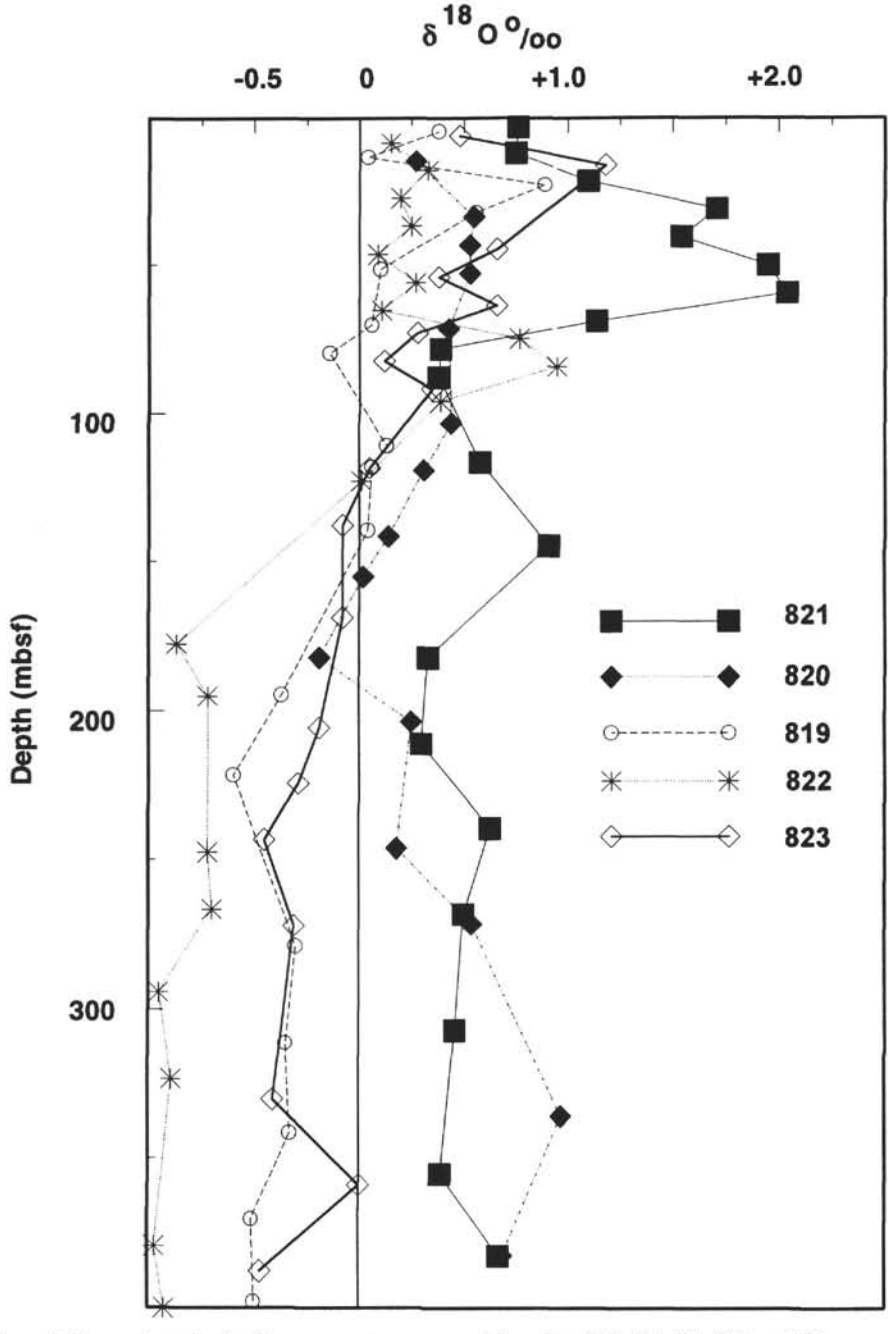

Figure 3. Oxygen isotopic data from pore waters recovered from Sites 819, 820, 821, 822, and 823.

Diffusion from an underlying saline source is neither supported nor refuted by stable O and C isotopic data. At Site 815, the $\delta^{18}O$ is isotopically enriched throughout the entire core and shows no significant changes in the lower portion of the core corresponding to the salinity increase. The $\delta^{13}C$ exhibits a slight increase in the lower samples. At Site 823, the $\delta^{18}O$ shows an increase in the lower portion, although this cannot be definitively ascribed to the chlorinity changes and may be a result of recrystallization at higher temperatures.

Site 823 exhibits perhaps the highest concentration of Sr^{2+} yet measured in pore waters from either the ODP or DSDP drilling. Concentrations as high as 2774 μM are reached at 934.6 mbsf. These fluids are still below celestite saturation, as the sulfate has been completely depleted. These high values are reached as a result of the relatively low permeability of the sediments, combined with the absence of sulfate and the continued recrystallization of the carbonate sediments.

Great Barrier Reef Margin Sites

Sites 822, 819, 820, and 821 form a distal-to-proximal transect off the eastern margin of the Queensland continental margin. The sediments are composed primarily of mixtures of periplatform carbonates derived from the Great Barrier Reef and quartz, feldspars, and clay minerals eroded from the Australian mainland. The concentration of clay minerals increases with increasing distance from the continental shelf, making up more than 50% of the sediments at Sites 819 and 820. Quartz usually composes between 10% and 20% of the sediments at each site, although the proximal sites have a slight tendency

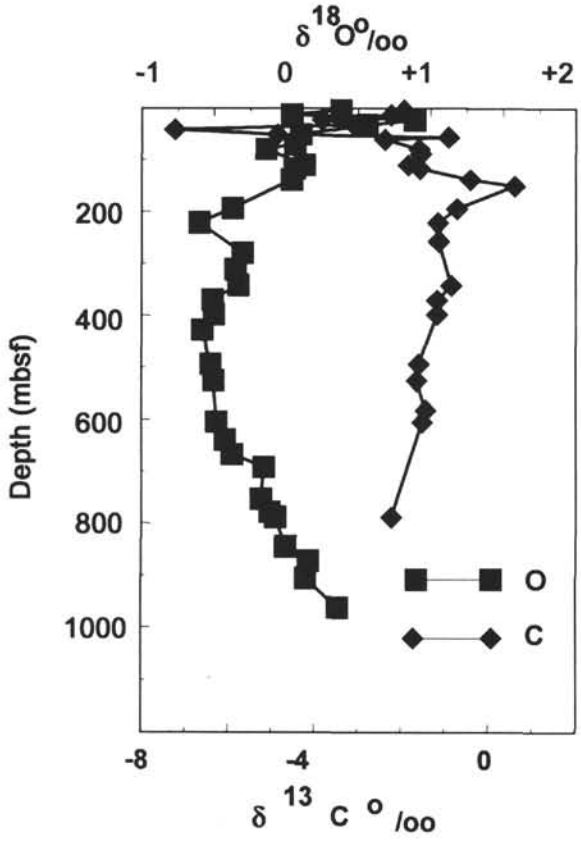

Figure 4. Oxygen and carbon isotopic data from pore waters from Site 823.

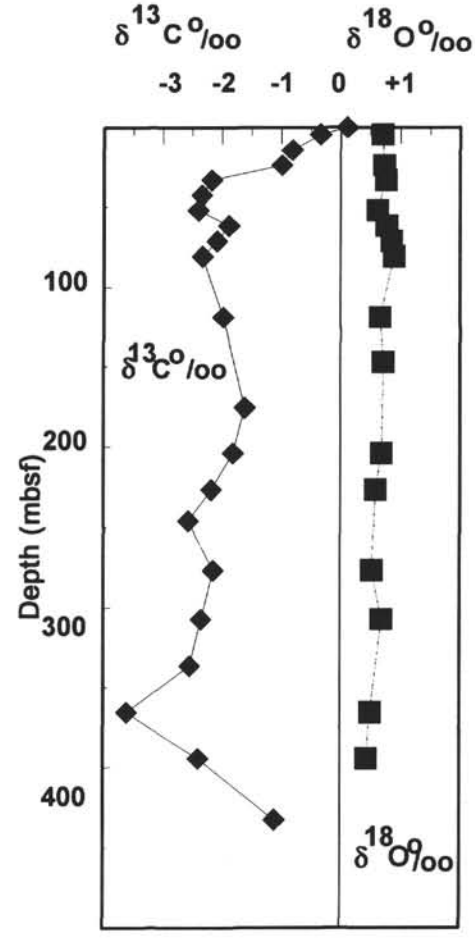

Figure 5. Oxygen and carbon isotopic data recovered from pore waters at Site 815.

to contain higher concentrations. The clay minerals mainly consist of kaolinite and illite, and the feldspars are principally albite.

Calcium, Magnesium, Potassium, Strontium, and Oxygen Isotopes

Decreases in the concentrations of K^+ and Mg^{2+} and increases in Na^+ concentration were attributed to the diagenesis of igneous minerals (Davies, McKenzie, Palmer-Julson, et al., 1991). In addition, data presented in this study show a depletion in $\delta^{18}O$ in the pore fluids. In previous work, depletions in the concentrations of K^+, Mg^{2+}, and $\delta^{18}O$, as well as increases in Ca^{2+}, have been attributed to alteration of Layer 2 basalts or volcanic material within the sediments to clay minerals or zeolites at elevated temperatures (Lawrence et al., 1976; Perry et al., 1976). As the Leg 133 sites are not located immediately over basement, reactions responsible for the depletion in Mg^{2+}, K^+, and $\delta^{18}O$ and the decrease in Ca^{2+} must be taking place within the sediments (Fig. 13). Because the maximum temperature of the sediments cored is probably less than 50°C, it is unlikely that the alteration of clay minerals, as originally suggested (Davies, McKenzie, Palmer-Julson, et al., 1991), can be invoked to account for the geochemical changes observed in the pore waters. One possible explanation for the decrease in K^+ and increase in Na^+ involves absorption and desorption from illite (Hoffman, 1979). Although changes in the $\delta^{18}O$ of the pore waters then could be explained by the alteration of volcanic glass, the observed decrease also could be a result of recrystallization of the relatively isotopically light precursor carbonate in colder waters. For example, Figure 14 shows the evolution of pore water in a closed system as it is subject to carbonate recrystallization. The equations used to construct these plots have been taken from Killingley (1983). In each of the three cases, the isotopic composition of the initial water has been set at +0.5‰ standard mean ocean water (SMOW), the bottom temperature at 10°C, and the geothermal gradient at 57°C/km (data taken from Davies, McKenzie, Palmer-Julson, et al., 1991). It is assumed that 100% recrystallization occurs by 400 mbsf and that once carbonate has been recrystallized it no longer reacts with the pore fluid. The difference among the three lines in Figure 14 represents differing isotopic compositions of the precursor. As may be observed, each case shows a depletion with depth. These calculations are in some ways similar to the measured data shown in Figure 3. Obviously, some discrepancies exist, such as the elevated isotopic composition at Site 821. This may be a result of fossil water trapped in the sediment. In addition, Site 821 exhibits the steepest Sr^{2+} gradients and, hence, the highest amount of carbonate recrystallization. However, this site does not exhibit as significant a depletion in the $\delta^{18}O$ as at Sites 819 and 822, which on the basis of their Sr^{2+} gradients should show lower rates of recrystallization. Explanation for these differences may lie in the different isotopic composition of the precursor, differences in the isotopic composition of the water, differences in the rate of recrystallization, and even some degree of alteration of volcanic glasses.

All the continental margin sites have heavy $\delta^{18}O$ values in the upper 50 to 100 mbsf. We think that these heavy values are related to the original isotopic composition of the pore fluids formed on the adjacent continental shelf area.

Oxidation of Organic Material

The rapid rate of sedimentation at Sites 819 to 822 (100 to 200 m/m.y.) has resulted in the burial of organic material that has been subsequently oxidized by sulfate-reducing bacteria to produce H_2S and CO_2. In turn, these gases have been instrumental in the precipitation of pyrite, dolomite, and calcium carbonate. As the types and

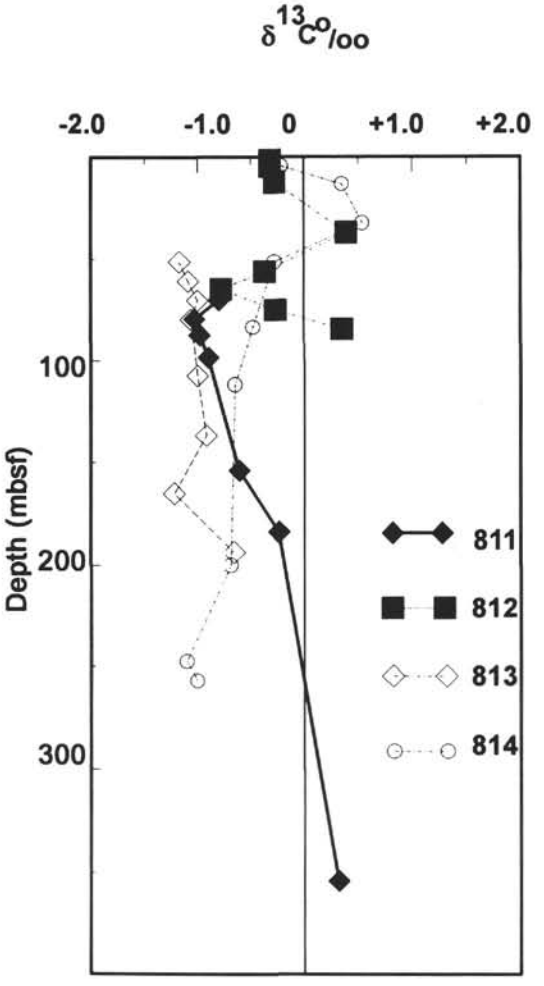

Figure 6. Carbon isotopic data from pore waters at Sites 811 through 814.

amount of minerals and organic material vary with distance from the shelf, the nature and magnitude of the diagenetic reactions occurring in the sediments also change, producing distinctive differences in the profiles of the interstitial minor elements at the four sites.

The most dramatic change visible at all sites is the removal of sulfate during the processes of organic material oxidation (Fig. 7). Although complete sulfate reduction occurs at all sites, it takes place as shallow as 25 mbsf at Sites 822 and 819, while at Site 821, sulfate is not completely exhausted until 144.5 mbsf. Small amounts of sulfate detected in the pore fluids below the sulfate depletion zone are thought to be a result of contamination. As all sites have experienced approximately similar rates of sedimentation and do not exhibit significant differences in their physical properties (permeability, density etc.), the most plausible explanation for the different depths of sulfate reduction lies in the different amounts and types of organic material present at each site. Sites 819 and 822 must have initially contained higher concentrations of organic matter or material that was more easily degraded than that at Sites 821 and 820. This initial difference is reflected in the present content of organic material at these sites; the organic material increases with increasing distance from the continental shelf. A further possibility is that, because the organic material at Sites 819 and 822 is predominantly of a marine rather than a terrestrial origin, it is more easily degraded by sulfate-reducing bacteria. Such a difference would promote higher rates of sulfate reduction at the distal sites. The difference in the rate of sulfate reduction is partially reflected in the variations in alkalinity, with the highest values occurring at Sites 819 and 822. The increase in alkalinity at these sites, however, is significantly less than that which might be expected as a result of sulfate reduction alone. This alkalinity deficit can be explained by: (1) the precipitation of dolomite and calcite; (2) loss of H_2S during the precipitation of pyrite.

Beneath the zone of sulfate reduction, large increases occur in the concentrations of methane. It has been suggested that these changes in the concentration might influence the $\delta^{13}C$ of the DIC and the consequent isotopic composition of diagenetic calcite and dolomite. However, although there were small depletions in the $\delta^{13}C$ of the DIC, there were no large changes as might have been expected based on the theories of Irwin et al. (1977) (Fig. 7). In fact, the most negative values in the sulfate reduction zone occurred at Site 819, and the smallest depletions at Site 821. It has been suggested that the absence of negative isotopic compositions resulted from the system being heavily buffered by carbonate minerals (Swart, this volume).

The magnitude of the increase in the concentration of Sr^{2+} in the interstitial fluids is often considered to be an indicator of the degree of carbonate recrystallization. If this is the case, then the amount of carbonate crystallization increases from the distal toward the proximal sites (Fig. 9). This observation supports the interpretation of the carbon isotopic data, which shows the smallest depletion in $\delta^{13}C$ at the proximal sites in the sulfate reduction zone and the smallest enrichment in the methanogenesis zone. Hence, the greater depletion in $\delta^{13}C$ seen at the distal sites and the higher isotopic compositions attained in the lower portions suggest that carbonate recrystallization is less important at these sites.

Accompanying these changes in pore-water chemistry is an increase in the concentration of dolomite from the distal to proximal sites (Davies, McKenzie, Palmer-Julson, et al., 1991). Therefore, the sites having the greatest degree of sulfate reduction and the highest alkalinity have the lowest concentrations of dolomite. Such a distribution is contrary to current hypotheses (Baker and Kastner, 1981) that dolomitization may be favored by high concentrations of alkalinity and low amounts of sulfate (Swart, this volume).

CONCLUSIONS

Pore fluids from Leg 133 can be separated into three groups on the basis of the processes that are postulated to control their composition.

1. Pore fluids from the Queensland Plateau sites are characterized by an absence of geochemical gradients, by modern strontium isotopic ratios, and, in some instances, by unusual geothermal gradients. These suggest the presence of significant fluid flow through the Queensland Plateau. The absence of a depletion in the $\delta^{18}O$ value of the pore waters and the slightly negative $\delta^{13}C$ values support the interpretation of fluid movement. The deeper flank sites (Sites 817 and 818) do not show evidence of fluid movement through the upper periplatform portion of the section. However, at Site 817, an underpressured zone was drilled that caused water to be drawn into the hole during drilling, suggesting the penetration of a fluid conduit.

2. The deeper trough sites (Sites 815 and 823) have exhibited diffusive control of pore-water constituents, combined with significant amounts of carbonate recrystallization. In the lower portion of the section, chloride concentrations increased together with the concentrations of various other constituents. These increases suggest the presence of an underlying evaporite unit. Such increases also were visible in the lower portions of Sites 817 and 818.

3. The Queensland continental margin sites are characterized by increasing rates of carbonate mineral diagenesis toward the Great Barrier Reef. In spite of total sulfate reduction and high rates of methanogenesis at these sites, little evidence could be ascertained of these processes in the $\delta^{13}C$ of the pore waters or in the isotopic composition of the diagenetic minerals. The isotopic signatures of sulfate reduction and methanogenesis were more evident in the distal sites. Although significant depletion in the Ca^{2+}, Mg^{2+}, K^+, and $\delta^{18}O$ content of the pore fluids was seen, only a decrease in K^+ and an

increase in Na^+ can be ascribed to interaction with clay minerals or formation of clay minerals from volcanic glasses.

ACKNOWLEDGMENTS

The authors would like to thank the technicians, scientists, and crew of Leg 133 for continued help throughout the cruise. Joe Powers, Joe DeMorett, and Scott Chaffey are especially thanked for their help in the chemistry laboratory. Help with the analyses was provided by Amel Saied, Jim Leder, Jeff Abell, Michel Lopez, and Phil Kramer. This paper benefited by reviews from Lynton Land and Joris Gieskes.

REFERENCES*

Baker, P.A., and Kastner, M., 1981. Constraints on the formation of sedimentary dolomite. *Science,* 213:215–216.

Davies, P.J., McKenzie, J.A., Palmer-Julson, A., et al., 1991. *Proc. ODP, Init. Repts.,* 133: College Station, TX (Ocean Drilling Program).

Ericson, E.K., 1976. Capricorn Basin. *In* Leslie, R.B., Evans, H.J., and Knight, C.L. (Eds.), *Economic Geology of Australia and Papua New Guinea* (Vol. 3). Australas. Inst. Mining and Metall. Monogr., 7:446–450.

Gieskes, J.M., Elderfield, H., and Palmer, M.R., 1986. Strontium and its isotopic composition in interstitial waters of marine carbonate sediments. *Earth Planet. Sci. Lett.,* 77:229–235.

Hoffman, J.C., 1979. An evaluation of potassium uptake by Mississippi-River-borne clays following deposition in the Gulf of Mexico [Ph.D. dissert.]. Case Western Reserve Univ., Cleveland, OH.

Irwin, H., Curtis, C.D., and Coleman, M.L., 1977. Isotopic evidence for the source of diagenetic carbonates formed during burial of organic-rich sediments. *Nature,* 269:209–213.

Killingley, J.S., 1983. Effects of diagenetic recrystallization of $^{18}O/^{16}O$ values of deep-sea sediments. *Nature,* 301:594–597.

Lawrence, J.R., Gieskes, J.M., and Anderson, T.F., 1976. Oxygen isotope material balance calculations, Leg 35. In Hollister, C.D., Craddock, C., et al., *Init. Repts. DSDP,* 35: Washington (U.S. Govt. Printing Office), 507–512.

Perry, E.A., Jr., Beckles, E.C., and Newton, R.M., 1976. Chemical and mineralogical studies, Sites 322 and 325. *In* Hollister, C.D., Craddock, C., et al., *Init. Repts. DSDP,* 35: Washington (U.S. Govt. Printing Office), 465–469.

Schlager, W., and James, N.P., 1978. Low-magnesian calcite limestones forming at the deep-sea floor, Tongue of the Ocean, Bahamas. *Sedimentology,* 25:675–702.

Swart, P.K., and Burns, S.J., 1990. Pore-water chemistry and carbonate diagenesis in sediments from Leg 115: Indian Ocean. *In* Duncan, R.A., Backman, J., Peterson, L.C., et al., *Proc. ODP, Sci. Results,* 115: College Station, TX (Ocean Drilling Program), 629–645.

Swart, P.K., and Guzikowski, M., 1988. Interstitial-water chemistry and diagenesis of periplatform sediments from the Bahamas, ODP Leg 101. *In* Austin, J.A., Jr., Schlager, W., Palmer, A.A., et al., *Proc. ODP, Sci. Results,* 101: College Station, TX (Ocean Drilling Program), 363–380.

* Abbreviations for names of organizations and publications in ODP reference lists follow the style given in *Chemical Abstracts Service Source Index* (published by American Chemical Society).

Date of initial receipt: 21 September 1992
Date of acceptance: 20 January 1993
Ms 133SR-258

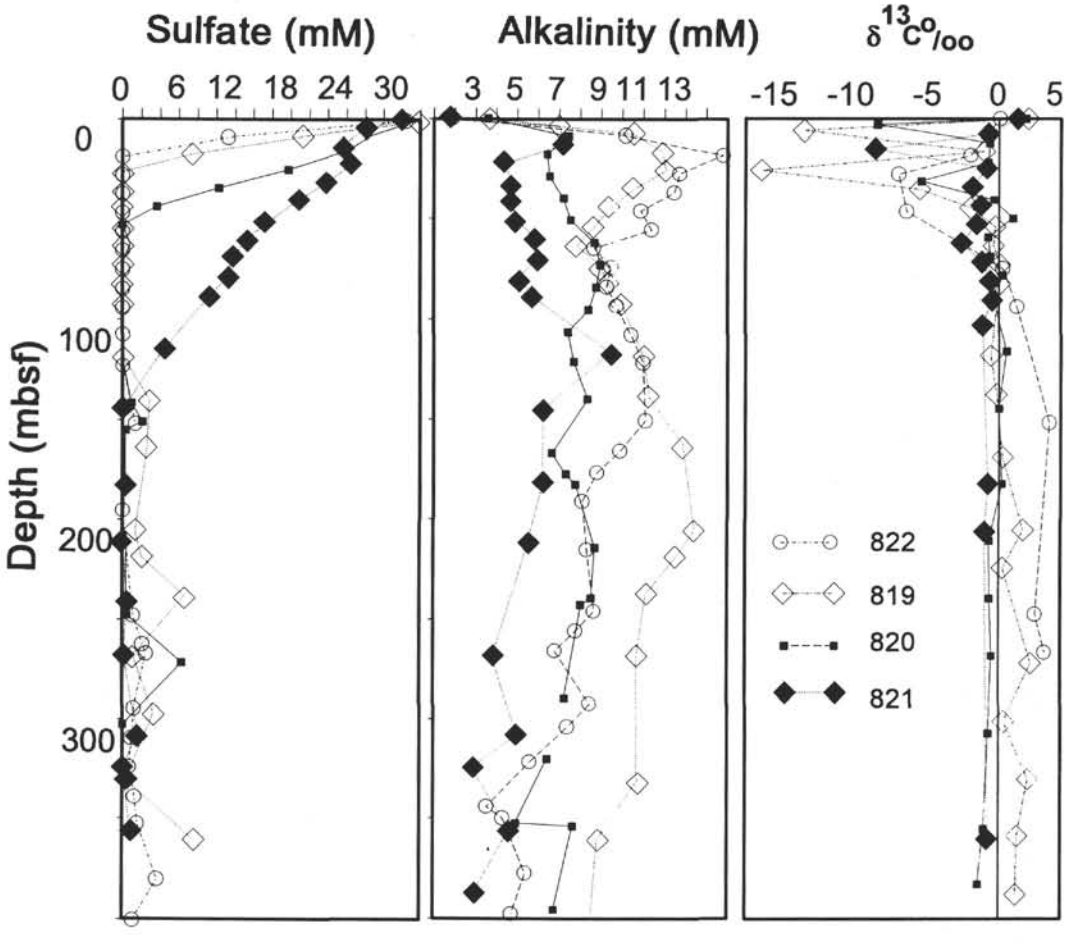

Figure 7. Sulfate, alkalinity, and carbon isotopic data from pore waters at Sites 819 through 822.

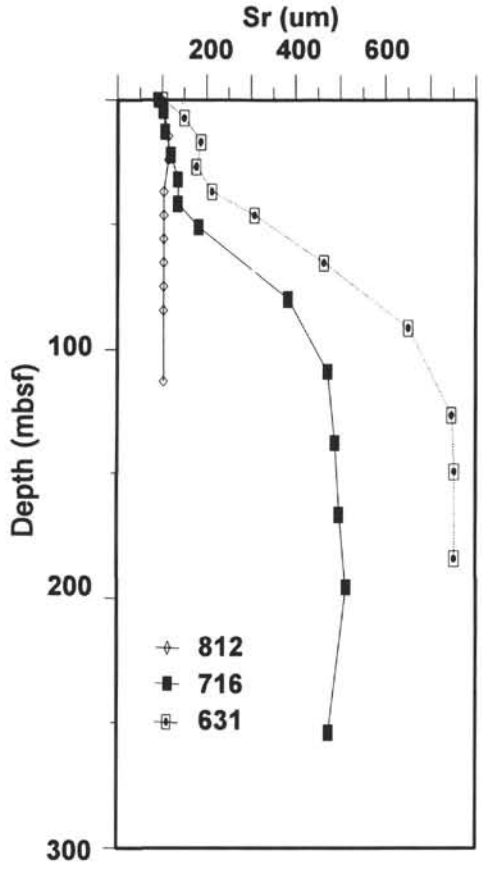

Figure 8. A comparison of the changes in the concentration of Sr^{2+} at Site 631 (Leg 101, Swart and Guzikowski, 1986), Site 716 (Leg 115, Swart and Burns, 1988), and Site 812 (Leg 133). Note the absence of an increase in Sr^{2+} at Site 812 compared with the other two sites.

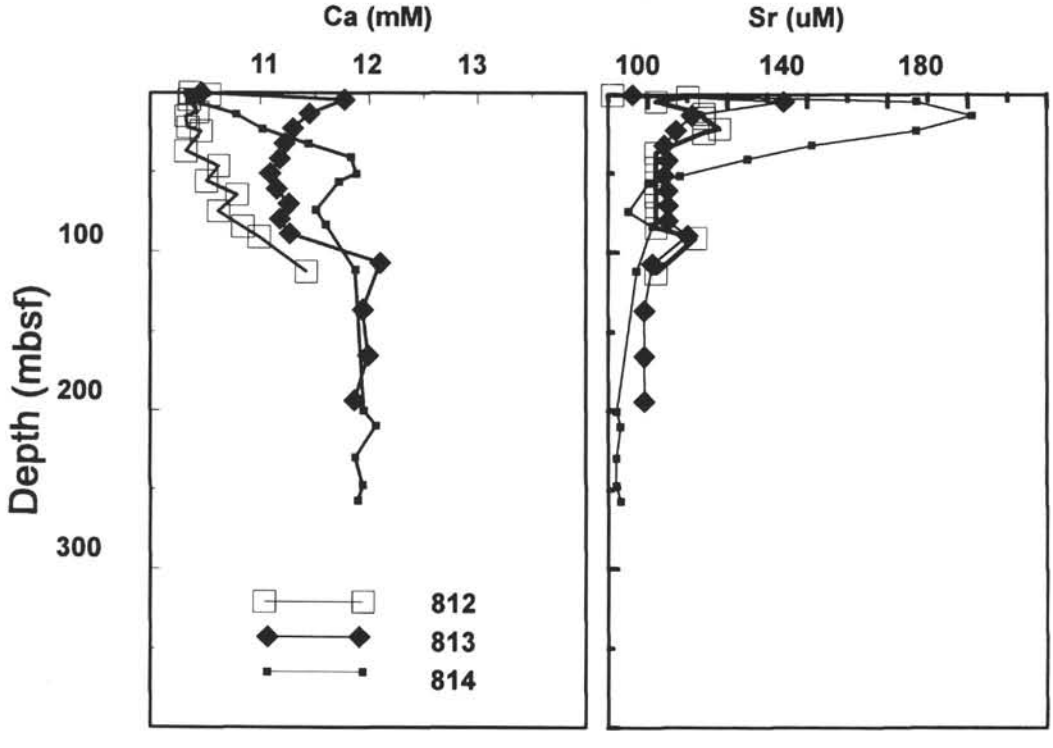

Figure 9. Interstitial pore-water calcium and strontium gradients from Sites 812 through 814.

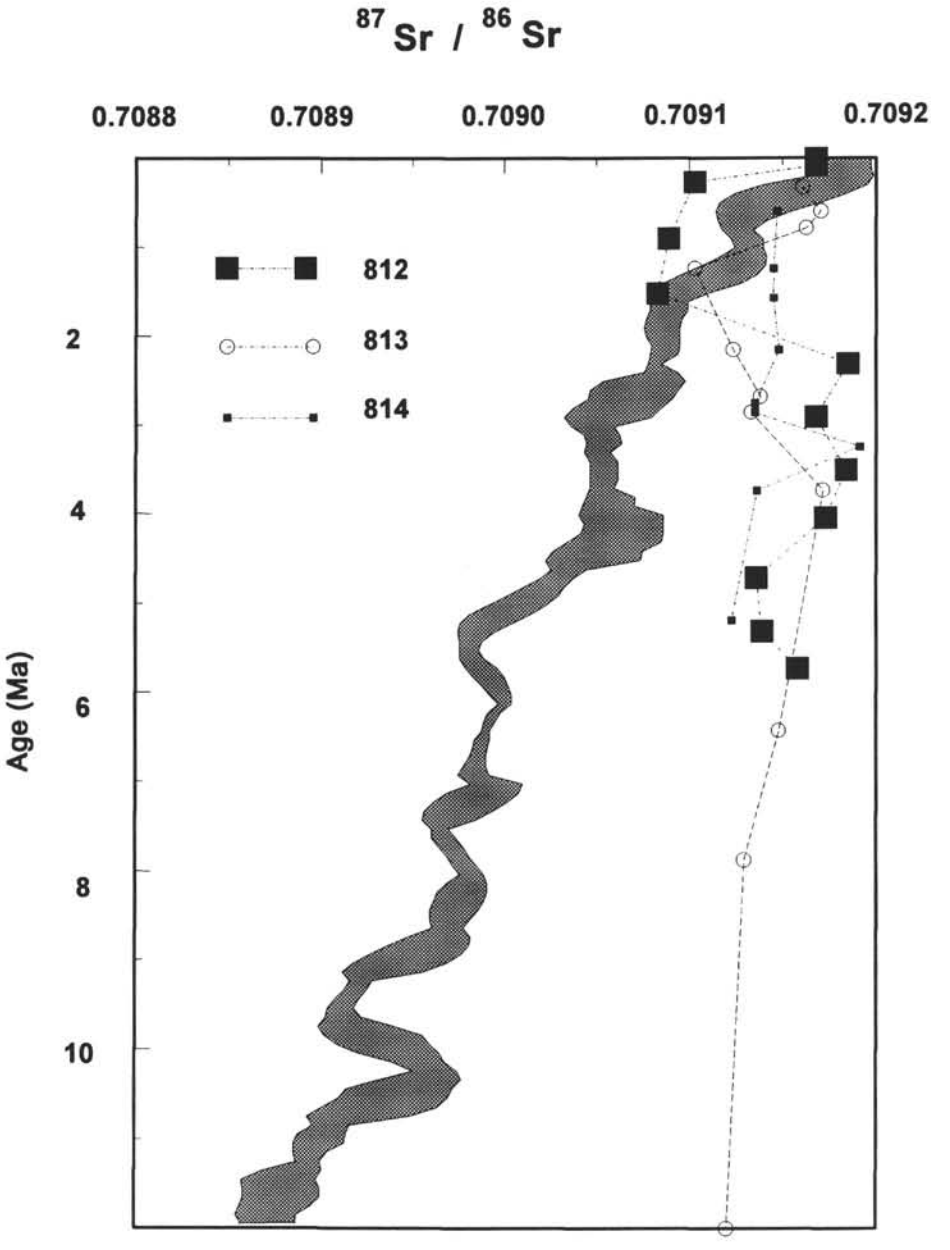

Figure 10. Strontium isotopic data from Sites 812 through 814 compared to contemporaneous seawater curve (gray shading). Note that most values are more radiogenic than contemporaneous seawater and are close to modern seawater values, suggesting circulation through the sediments (data from Elderfield et al., this volume). Dissolved Sr^{2+} profiles are shown in Figure 9.

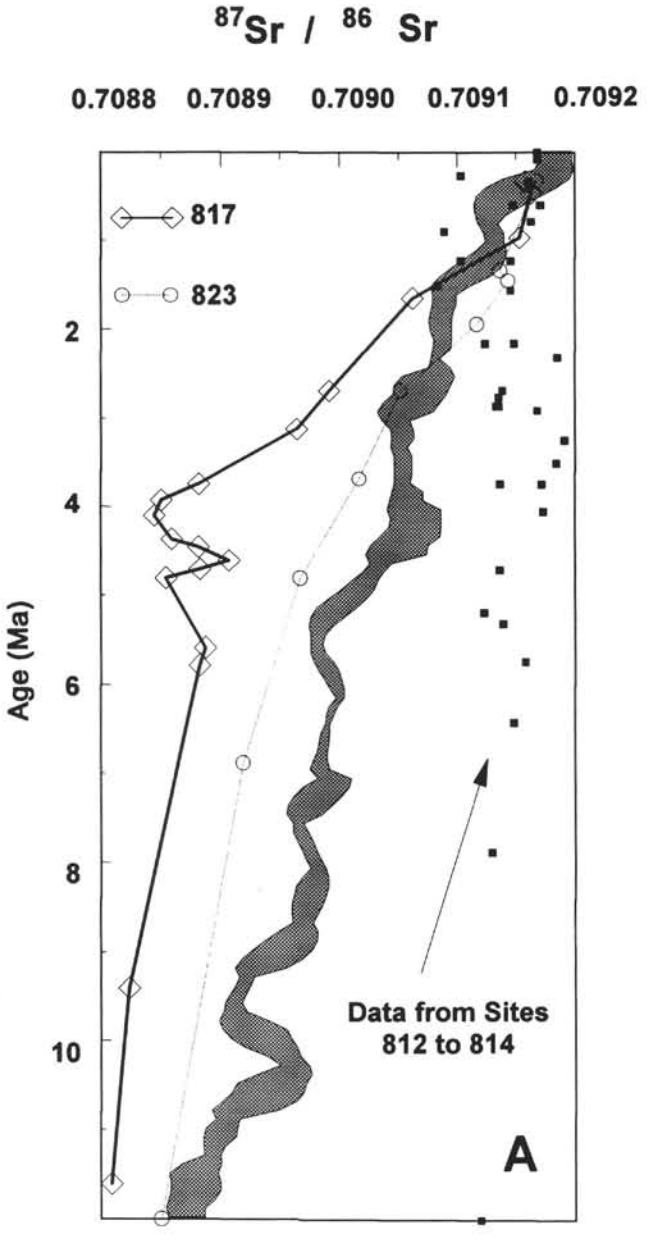

Figure 11. **A.** Strontium isotopic data from Sites 817 and 823 compared to contemporaneous seawater curve (data from Elderfield et al., this volume). Also shown are data from Figure 9 for comparison. Strontium isotopic data fall below the seawater curve, in contrast to data from Sites 812 to 814. **B.** Strontium concentration data from Sites 817 and 823.

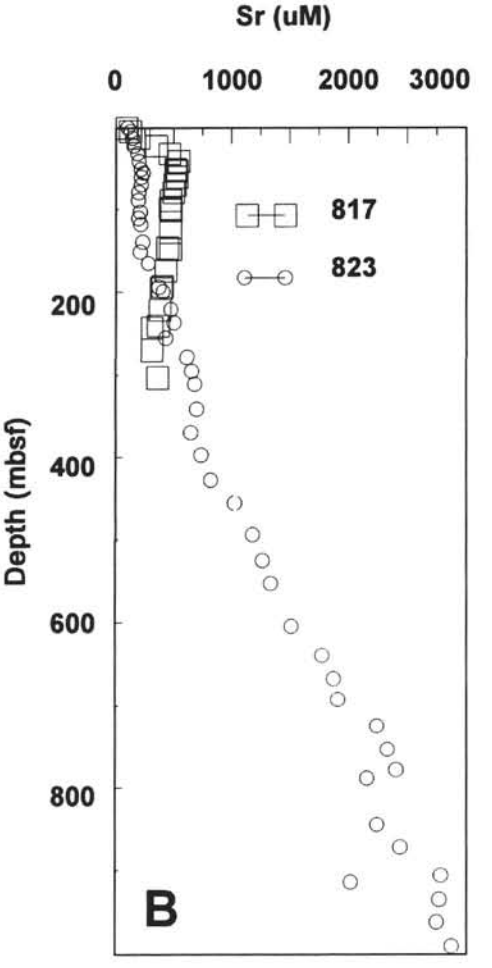

Figure 11 (continued).

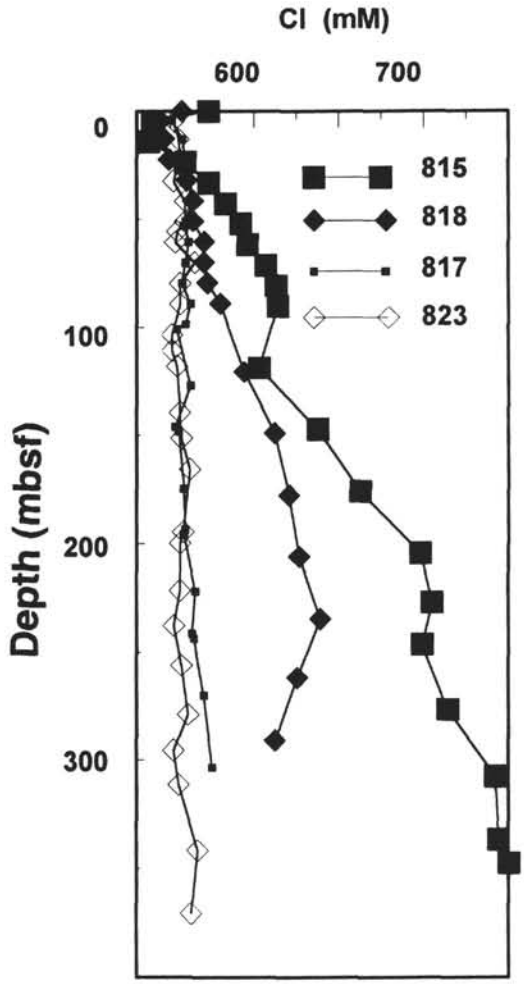

Figure 12. The concentrations of Cl^- at Sites 815, 817, 818, and 823. All sites exhibit a general increase in the lower portions of the hole.

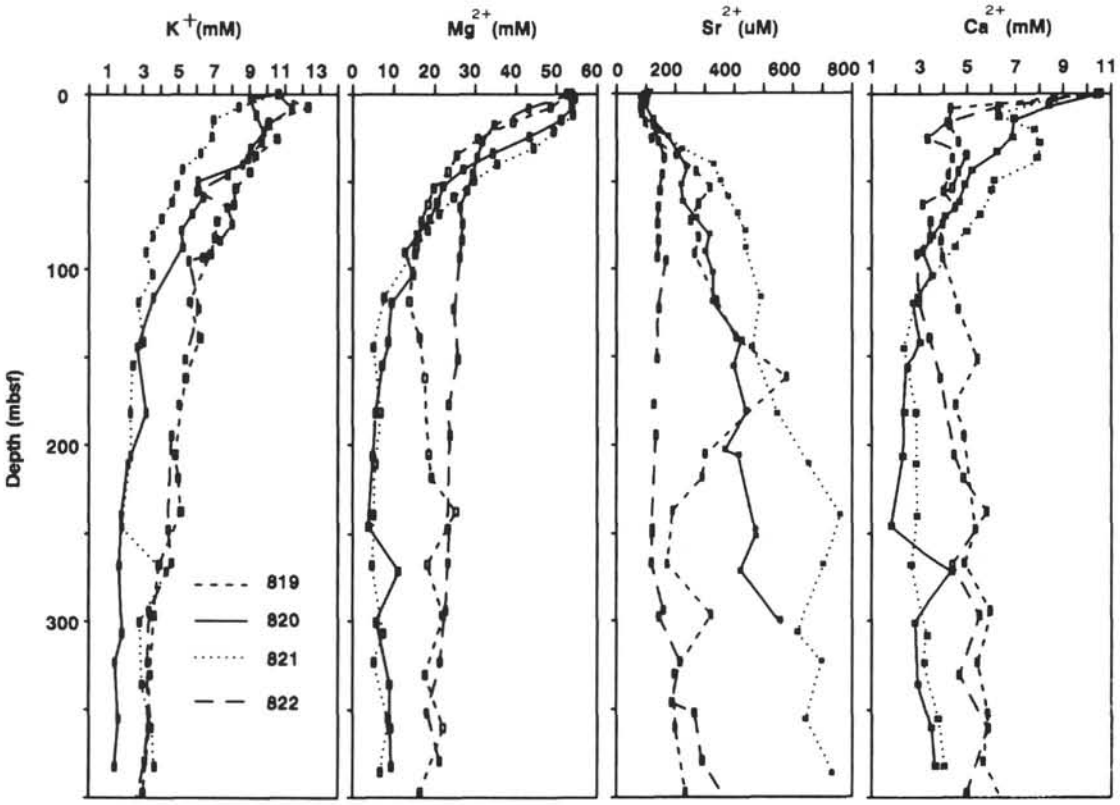

Figure 13. Changes in the concentrations of K^+, Mg^{2+}, Sr^{2+}, and Ca^{2+} at Sites 819 through 822.

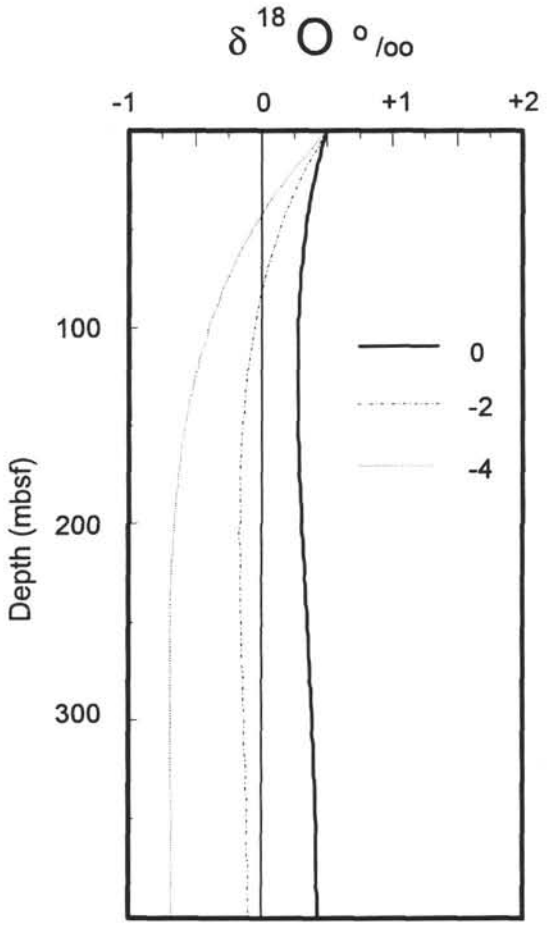

Figure 14. Hypothetical changes in the $\delta^{18}O$ of pore waters with depth as a result of recrystallization of carbonates having different initial isotopic compositions. Note the similarity of the changes to the measured data in Figure 3.